JOURNAL OF GEOPHYSICAL RESEARCH, VOL. 105, NO. E5, PAGES 11,999–12,022, MAY 25, 2000

Characteristics and origin of polygonal terrain in southern Utopia Planitia, Mars: Results from Mars Orbiter Laser Altimeter and Mars Orbiter Camera data

Harald Hiesinger and James W. Head III

Department of Geological Sciences, Brown University, Providence, Rhode Island

Abstract. Giant polygons on Mars with several kilometers in diameter were first observed in Mariner 9 and Viking Orbiter images, and their origin, formation, and evolution have remained enigmatic since that time. New data obtained by the Mars Orbiter Laser Altimeter (MOLA) and the Mars Orbiter Camera (MOC) on board the Mars Global Surveyor spacecraft now permit analysis of topography and morphology of the polygonal terrain in unprecedented detail. MOLA data show that (1) giant polygonal terrain in Utopia is located at the lower slopes of a basin structure, that is the Utopia basin; (2) the onset of polygonal terrain in Utopia is close to the same elevation in several profiles and lies at about the same elevation as a terrace which was interpreted as a shoreline of an ancient body of standing water within the Utopia basin proper; (3) polygonal terrain occurs over a wide range of elevations on regional slopes of ~0.1°; (4) the depths of the troughs range from <5 m to 115 m, averaging about 30 m, and tend to be greater toward the center of the Utopia basin; (5) the mean width of polygonal troughs is of the order of 2 km, ranging from <0.5 to 7.5 km. Data from the Mars Orbiter Camera (MOC) indicate that (1) the troughs are generally broad graben-like features with varying morphologies (i.e., terraces and lobateness) and dimensions (widths and depths); (2) trough morphology has been modified by aeolian processes; (3) polygonal troughs are weakly interconnected at MOC resolutions and there are no smaller polygons observed within the giant polygons; (4) circular depressions which are probably related to subsurface collapse sometimes occur at the bottoms of polygonal troughs; (5) small-scale polygonal terrain on the ejecta blankets of young craters with fluidized ejecta in the investigated area exhibits different characteristics (i.e., smaller size, presence of rims, greater degree of interconnections) than giant polygons. In the Viking images we see that (1) old impact craters are increasingly buried with younger materials toward the basin center and that (2) a large number of superposed impact craters on polygonal terrain exhibit distinctive ejecta morphologies such as rampart ejecta blankets and single and double lobate ejecta blankets. MOLA and MOC observations are consistent with the formation of polygonal terrain in the area of a former standing body of water, but polygon size seems too large to be readily accounted for by desiccation or freezing processes alone. On the basis of the observed characteristics we propose that the giant polygons are primarily of tectonic origin, being caused by uplift of the floor of the Utopia basin. There are several candidates for the cause of uplift: (1) the removal of the load representing former standing bodies of water. Water thickness estimated for the Utopia basin is about 1 km. In this scenario, removal of this load (comparable to loads placed on terrestrial continental lithosphere by the Laurentide and Scandinavian ice sheets) by loss of the water or ice could cause uplift of the floor and polygon formation. (2) The freezing and expansion of residual water buried by sediments or in the near subsurface, or (3) a combination of these. From the discussion of alternative models in the light of the MOLA and MOC data we conclude that formation of giant polygons by tectonic uplift of the basin floor is most likely and deserves further investigation.

1. Introduction

Giant polygonal terrain is a major morphologic constituent of the Utopia Planitia region of the northern plains on Mars. These polygons formed during the Late Hesperian [*Scott and Tanaka*, 1986; *Greeley and Guest*, 1987] and are thought to be in close genetic relation to outflow channels and a possible ancient Martian ocean [*Lucchitta et al.*, 1986; *Parker et al.*, 1989]. However, it is still under discussion what kind of process formed polygonal terrain and whether polygonal terrain formed on volcanic or sedimentary deposits. We address these questions and test previously published models in the light of the new Mars Orbiter Laser Altimeter (MOLA) [*Smith et al.*, 1998] and Mars Orbiter Camera (MOC) [*Malin et al.*, 1998] data.

Numerous models have been suggested for the formation of polygonal terrain on Mars and all models involve cracking in response to tension. Tension-generating processes are (1) loading of sediments with volatile-rich lavas [*Helfenstein and Mouginis-Mark*, 1980; *Needham*, 1978], (2) cooling of lava flows [*Masursky and Grabill*, 1976; *Carr et al.*, 1976; *Morris*

Paper number 1999JE001193
0148-0227/00/1999JE001193$09.00

and Underwood, 1978], (3) coalescence of smaller polygons [*Helfenstein and Mouginis-Mark*, 1980], (4) tectonic processes [*Mutch et al.*, 1976], (5) tectonic bending over a rough subsurface [*McGill and Hills*, 1992], (6) convection [*Wenrich and Christensen*, 1993, 1996], (7) thermal contraction [*Carr and Schaber*, 1977], and finally (8) desiccation of wet sediments [*Morris and Underwood*, 1978]. We review these models, their predictions and constraints, and describe key characteristics of midlatitude (27°-39°N, 247°-265°W) Martian polygonal troughs in southern Utopia Planitia which allow us to test the plausibility of each model. Key characteristics of troughs are the location relative to the Utopia basin structure [*McGill*, 1989; *Frey and Schultz*, 1990; *Schultz and Frey*, 1990; *Thomson and Head*, 1999], morphometry (width, depth, and dip angle), morphology, and topography.

As all of the models for the formation of polygonal terrain are more or less dependent on these parameters, MOLA and MOC offer a unique opportunity to contribute to the discussion of the models for the formation of Martian polygons. MOLA and MOC can provide major contributions such as the characterization of polygons in relation to the regional topography, the morphology, the detailed description of trough morphometry, as well as the quantification of local and regional slopes on which polygonal terrain is exposed. Therefore MOLA and MOC are excellent tools in order to investigate the key characteristics of polygonal terrain, to discuss the models, and to test their predictions.

2. Characteristics of Polygons: The Pre-Mars Global Surveyor (MGS) View

Giant polygons are relatively common on the northern plains of Mars. Most of them are located in southeastern Acidalia Planitia (45°N, 15°W), northwestern Elysium Planitia (36°N, 256°W), and Utopia Planitia (49°N, 233°W) [*Pechmann*, 1980]. However, polygons comparable in size and morphology were also found in very limited areas at the junction of Ius Chasma and Tithonium Chasma [*Blasius et al.*, 1977] as well as in small areas northwest of Kasei Vallis. Additional polygonal terrain was identified in regions north of 70° latitude [*Squyres et al.*, 1992]. Polygons in this region are outlined by subtle depressions and exhibit a different morphology than the polygons elsewhere in the northern plains [*Pechmann*, 1980]. *Lucchitta et al.* [1986] noted that polygonal terrain generally occurs in close proximity to the major outflow channels and in low reentrants of the northern lowlands projecting into the southern highlands (Plate 1). According *to Lucchitta et al.* [1986], these reentrants may have served as bays to accumulate wet sediments emplaced in channel-forming events from the southern highlands. The size of giant Martian polygons is in the range of 2-32 km [*McGill*, 1986, 1987; *Pechmann*, 1980; *Lucchitta*, 1983; *Helfenstein and Mouginis-Mark*, 1980; *Borrello*, 1987]. *Helfenstein and Mouginis-Mark* [1980] measured the size of 383 polygons in Utopia, Acidalia, and the polar regions and found that the largest polygons tend to occur in Utopia (mean size 7.4 km) and the smallest in the polar regions (mean size 3.5 km). The width of the fractures which form giant polygons is about 200-800 m [*Pechmann*, 1980]. This is consistent with data from *McGill* [1986], which indicate a width of 250-1000 m with some fractures much larger than 1 km. According to *Morris and Underwood* [1978], the fracture width can vary up to 2 km. The depths of these fractures were based on shadow length measurements on Viking images. Based on data from D. W. G. Arthur, *Pechmann* [1980] noted that the depth of four representative troughs varies between 30±10 m and 107±10 m. *Morris and Underwood* [1978] mention that polygonal troughs are typically a few hundred meters deep. Based on investigations of buried impact craters, *McGill* [1987] proposed a thickness of the polygonal terrain unit of 500 m. In a more recent paper, *McGill and Hills* [1992] suggested a regional thickness of 600 m. These estimates are based on the observations of *Pike and Davis* [1984] that craters with diameters between 8 and 30 km have rims that rise 225-380 m above the intercrater surface and thus the layer to completely cover the crater rims must be about 400 m. For the formation of polygonal terrain, *McGill and Hills* [1992] assume that the layer thickness must be equal or greater than twice the depth of the troughs. Coupling these constraints with typical trough depths [*Pechmann*, 1980], they conclude that crater rims have to be buried by an additional 200 m thick layer, giving a thickness of 600 m for the polygonal terrain.

3. Characteristics of Polygons: The MGS View

In this chapter we will use new MOLA topographic data as well as MOC image data in order to study giant polygonal terrain. We will specifically investigate the geologic context, the relation to the regional topography within the Utopia basin, and the morphological characteristics (e.g., width, depth, and slopes) of giant polygons in order to test models of their origin.

In 1997 the laser altimeter (MOLA) on board the Mars Surveyor spacecraft started to acquire high-precision topographic profiles along near polar ground tracks in the northern hemisphere. The instrument has a vertical shot-to-shot resolution of ~30 cm, an absolute vertical precision of 10 m, and along-track spatial resolution of 300-400 m [*Smith et al.*, 1998]. The surface spot size in mapping orbit is about 130 m. These specifications allow one to resolve narrow graben- or fault-like features in the MOLA profiles. We have investigated the geometry of 169 troughs forming parts of the polygonal terrain of southern Utopia Planitia (unit Hvg and Hvg$_1$ in Figure 1). We focused on polygonal terrain in the latitude range between 27°N and 47.5°N and longitudes between 247.5°W and 270° W, an area that is mostly covered by the U.S. Geological Survey (USGS) photomosaics I-1427 and I-1432 (1:2M). For our investigation we made use of the data obtained during aerobraking (hiatus-orbits) and from the science phasing orbits

Plate 1. Distribution and examples of polygonal terrain in the northern lowlands. Central part is a Lambert azimuthal equal-area projection of the MOLA topography of the northern hemisphere. Viking image numbers are: (top left) 560B63 (~ 122 m/pixel resolution), (bottom left) 669B28 (~185 m/pixel resolution), and (right) mosaicked digital image models (MDIMs) (~230 m/pixel resolution). Polygonal terrain shows a wide variety in sizes and morphologies.

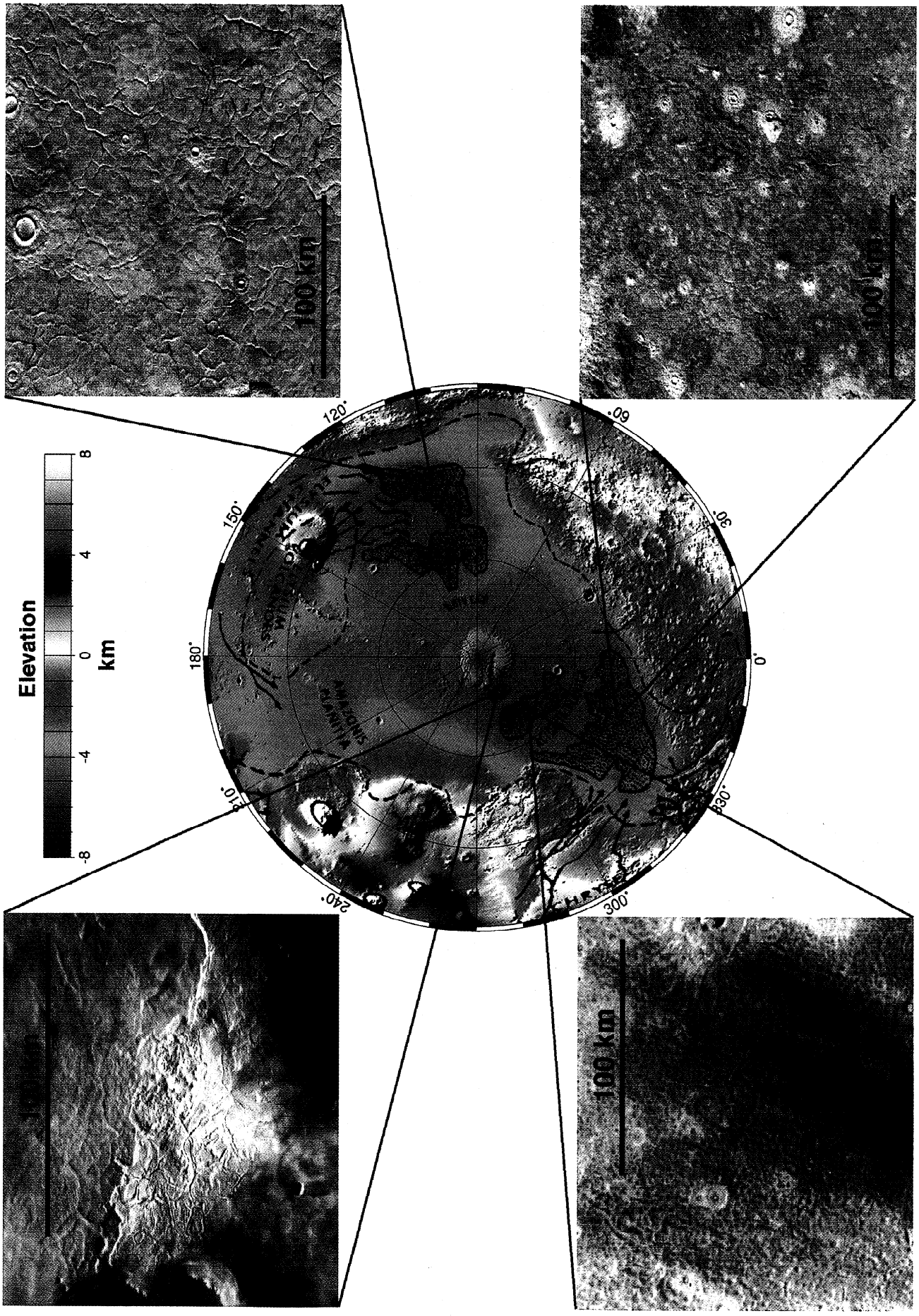
100 km
100 km
100 km
Elevation
km
8
4
0
-4
-8
120°
60°
150°
30°
180°
0°
210°
330°
240°
300°
ARABIA TERRA
AMAZONIS PLANITIA
HESPERIA

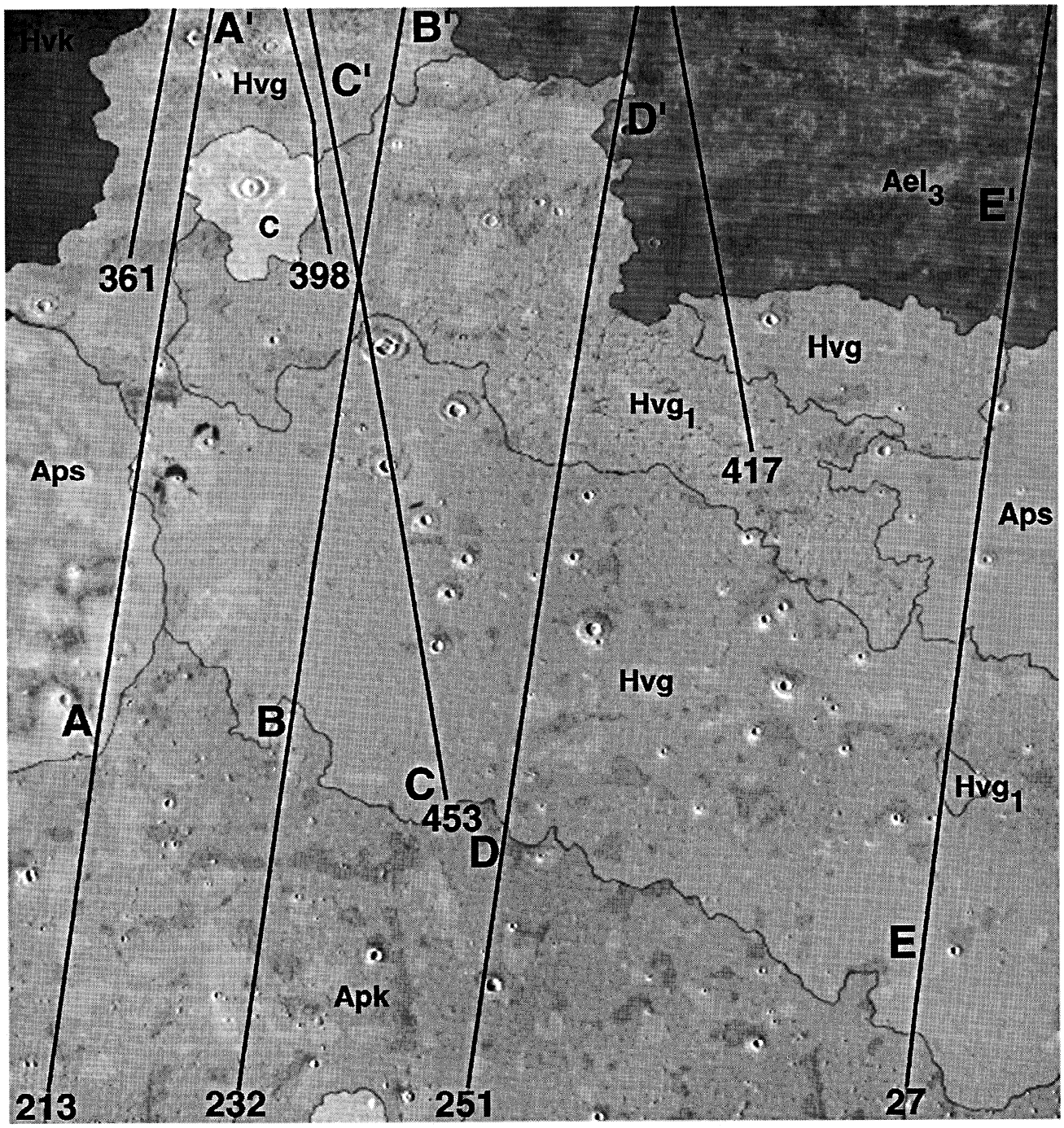

Figure 1. Viking Orbiter mosaic of the investigated area in southern Utopia Planitia with adapted geologic map from *Greeley and Guest* [1987]. Superposed are eight MOLA ground tracks. Letters indicate geologic units (Ael_3, member 3 of Elysium Formation; Apk, knobby plains material; Aps, smooth plains material; Hvk, knobby member of the Vastitas Borealis Formation; Hvg, grooved member of the Vastitas Borealis Formation; Hvg_1, intensely grooved member of the Vastitas Borealis Formation; c, impact crater material). The location of the profiles of Figure 3 are also shown (e.g., A-A').

(SPO1&2). The precision of MOLA data is continuously improved by globally minimizing errors between crossing MOLA tracks. This procedure provides versions of data, labeled in alphabetical order, with increasingly smaller errors. In this study we used data version m. Seven orbits were investigated in detail: 27, 417, 251, 453, 232, 213, and 361 (sorted by increasing longitude).

3.1. Location, Geologic Context, and Relation to Regional Topography

The geologic map [*Greeley and Guest*, 1987] shows that polygonal terrain in Utopia Planitia mainly consists of material of the Vastitas Borealis Formation which is of Hesperian age (Hvg, Hvg_1, Hvk in Figure 1). The Vastitas Borealis Formation

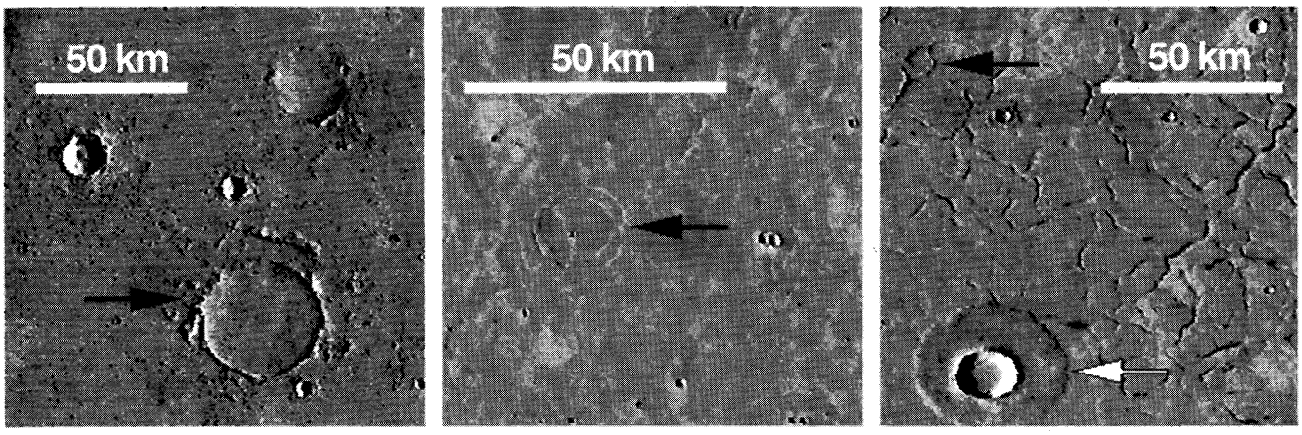

Figure 2. Examples of impact crater morphologies in Utopia Planitia. Black arrows indicate old impact craters, which are increasingly buried by younger material toward the basin center, that is, from left to right. White arrow points to a young crater with fluidized ejecta blanket, which postdates the polygonal terrain formation.

is of volcanic, alluvial, or aeolian origin and shows evidence of tectonism, compaction, or periglacial and erosional processes [*Greeley and Guest,* 1987]. The channeled deposits of the Ael_3 unit which are Amazonian in age are interpreted as lahar streams [*Christiansen*, 1989] which have flooded the basin center from the southeast and have partly covered the polygonal terrain. Using Viking mosaics with 230 m resolution, we mapped old impact craters in southern Utopia Planitia and found that they are increasingly buried with younger sediments toward the center of the Utopia basin, which is consistent with observations of *McGill and Hills* [1992] and *McGill* [1989]. We also see that young craters, which are superposed on polygonal terrain, show distinctive ejecta morphologies such as rampart ejecta blankets or single and double lobate ejecta blankets (Figure 2). *Head et al.* [1999] showed that the smallest craters with fluidized ejecta blankets occur in depressions within the north polar lowlands and are highly correlated with polygonal terrain. It has been proposed that these crater morphologies are caused by impact melting and/or vaporization of ground ice and groundwater [e.g., *Carr et al.,* 1977; *Mouginis-Mark,* 1979, 1981, 1986; *Kuzmin et al.,* 1988a, b; *Squyres et al.,* 1992; *Barlow,* 1994; *Costard and Kargel*, 1995]. Alternatively, fluidized ejecta morphologies have also been proposed to be caused by entrainment of Martian atmospheric gases [e.g., *Schultz and Gault,* 1979; *Barnouin-Jah and Schultz*, 1998].

Interpolating between all available MOLA orbits in order to generate a global topographic map [*Zuber et al.*, 1998] and combining this map with the map of *Lucchitta et al.* [1986] we find that the polygonal terrain in Utopia Planitia is located on the lower slopes of a topographic depression, that is, the Utopia basin proper [e.g., *McGill*, 1989; *Frey and Schultz*, 1990; *Schultz and Frey*, 1990; *Thomson and Head*, 1999]. Polygonal terrain north of the Chryse outflow channels which was mapped by *Lucchitta et al.* [1986] is also exposed in a large regional topographic low, that is, the north polar basin [*Smith et al.,* 1998]. In the USGS topographic map [*Eliason et al.,* 1992], which was available before MOLA, polygonal terrain was not as closely associated with topographic lows as in the new MOLA topographic map. In the USGS topographic map, polygonal terrain is exposed across ridges that define the northern closure of the Elysium basin and the Chryse basin in this map. Going northward along the five profiles that start south of the polygonal terrain, the onset of polygons occurs at about the same elevation level within a narrow range of ~70 m (-4339 m to -4410 m; Figures 3a-3e and 4). Polygonal terrain in the Utopia basin occurs at and below this elevation. In addition, the onset of polygonal troughs occurs close to the same elevation of a terrace at -4350 m [*Thomson and Head*, 1999]. *Thomson and Head* [1999] found that the terrace occurs at an elevation where a hypothetical water fill of the Utopia basin would spill over into the adjacent north polar basin and interpreted the terrace as a shoreline of a paleolake which once filled the Utopia basin (see their Figures 1 and 2). Five MOLA passes cross this terrace and in all passes the onset of polygonal troughs is within 60 m of the elevation of this terrace.

3.2. Slopes

Polygonal terrain in southern Utopia Planitia is tilted to the north and therefore follows the global trend observed in all MOLA profiles, independent of the geologic unit [*Smith et al.,* 1998, 1999; *Zuber et al.,* 1998]. This general trend shows a pronounced slope from higher elevations at the border to the southern highlands to lower elevations toward the pole, the north polar ice cap excluded. In other words, polygons occur at different topographic levels along the general north facing slope and do not mark a single horizontal topographic level.

Regional slopes were calculated as linear least squares fits of all data points. The slopes along the MOLA ground tracks in the investigated region are less than 0.1° over baselines of hundreds of kilometers and appear to be very similar for all investigated MOLA orbits. Orbit 417 shows the smallest slope (0.018°), orbit 251 the largest slope (0.063°), and orbit 27 (0.048°), orbit 213 (0.047°), orbit 232 (0.061°), orbit 361 (0.060°), and orbit 453 (0.046°) exhibit intermediate slopes. The mean slope of polygonal terrain in southern Utopia Planitia is 0.049°. These slopes are in excellent agreement with slopes measured by *Head et al.* [1998] who pointed out that the systematic slope from the equator to the pole in all profiles is of the order of 0.056°.

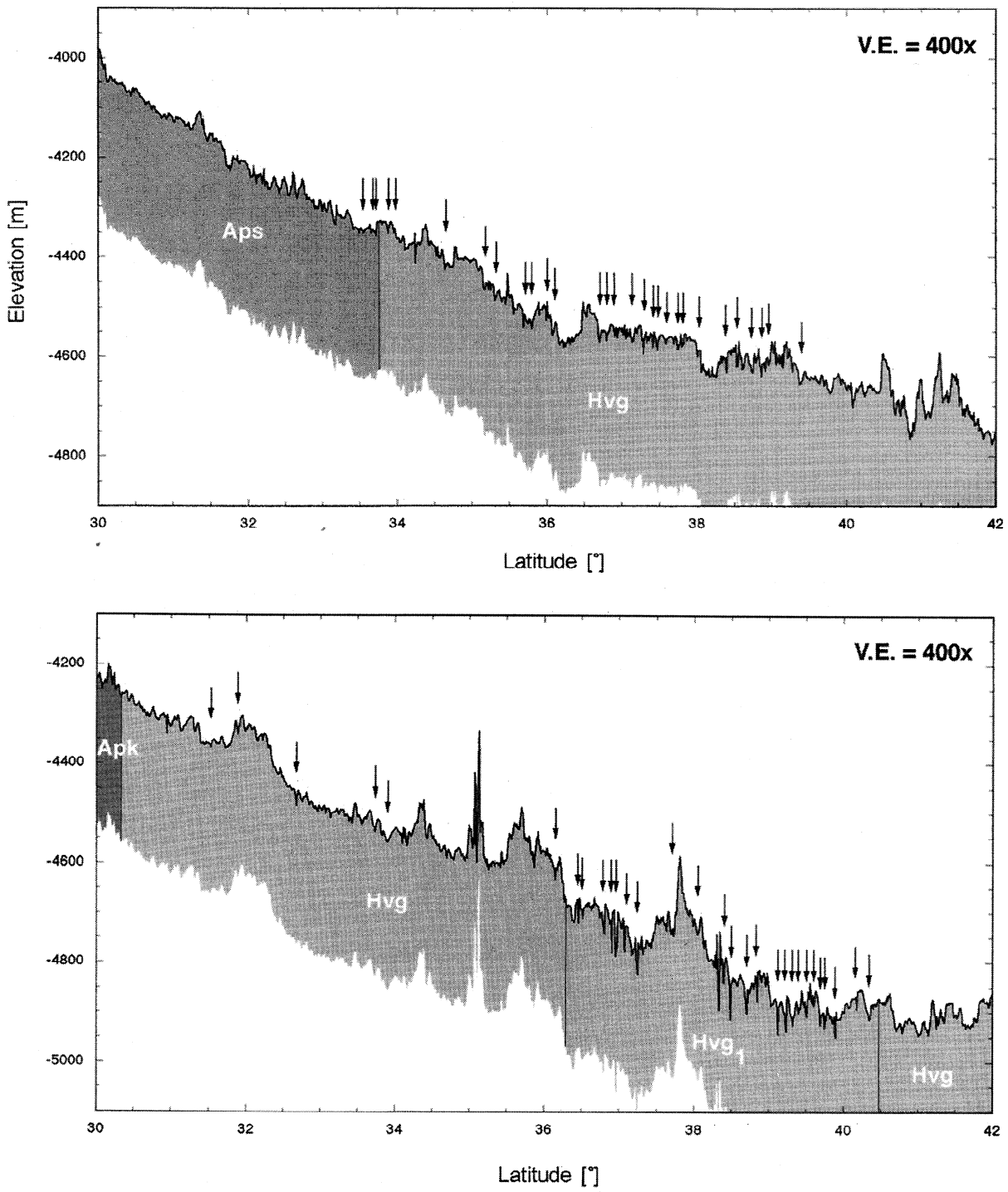

Figure 3. MOLA profiles crossing the investigated region in Utopia Planitia: (a) orbit 213, (b) orbit 232, (c) orbit 453, (d) orbit 251, and (e) orbit 27 showing the position of polygonal troughs (black arrows) in relation to topography and geologic units (see Figure 1 caption for unit designations). Geologic units are shown in different gray levels for better discrimination. V.E., vertical exaggeration.

3.3. Width, Depth, and Dip Angles

A crucial point in measuring widths and depths of fractures is the definition and interpretation of the fracture morphology. In other words, where and how to measure the fracture? In order to measure all polygonal troughs consistently, we have to define criteria for their measurements. This is not an easy task as the morphology of troughs can vary widely (e.g., sharp rims versus rounded rims) and can influence the measurement. In order to measure troughs in a self-consistent way, we determined the width of a trough at the highest possible point on the trough wall before the slope starts descending into an adjacent trough on either side of the measured feature. This means that the width of a trough was measured at a height that corresponds to the maximal hypothetical flooding of the trough before a fluid would spill over into the neighboring trough or depres-

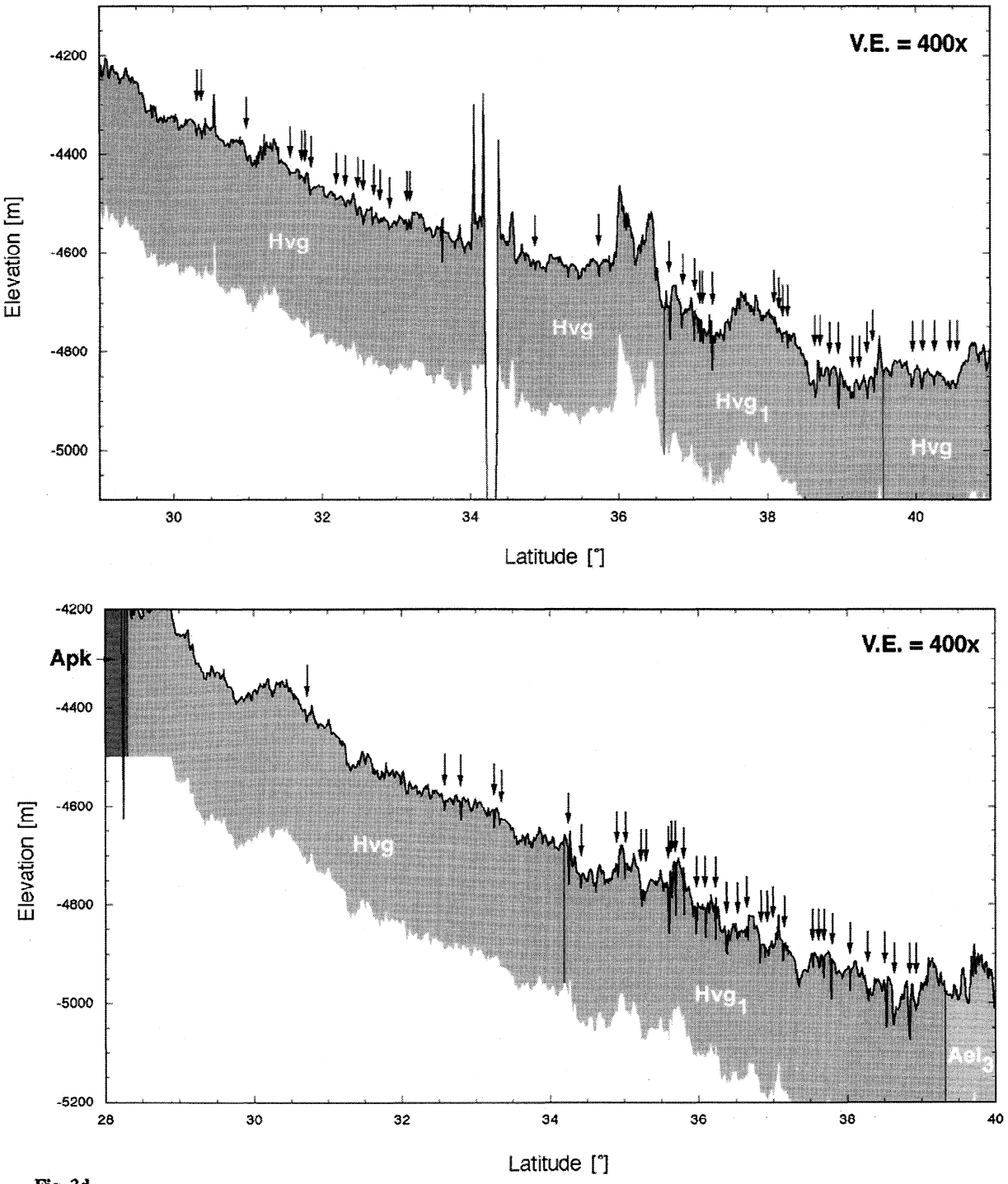

Fig. 3d

Figure 3. (continued)

sion (Figure 5). The depth of a trough was measured between this datum and the lowest point within the trough. MOLA profiles usually do not cross the polygon fractures perpendicularly. Therefore the width measured in the profiles has to be corrected for widening due to oblique cross cutting. Even after this correction our widths are considerably larger than previously published fracture widths of polygonal terrain of 200-800 m [*Pechmann*, 1980; *McGill*, 1986]. A large number of the investigated troughs exhibit rounded rims, an observation consistent with previously published trough morphologies [*Morris and Underwood*, 1978]. Illumination conditions of the Viking images ($i > 60°$) in combination with the morphology of the fractures could have led to a systematic underestimation of the polygonal trough widths in previous studies. The shot-to-shot distance of MOLA is of the order of 300-400 m [*Smith et al.*, 1998]. Therefore the definition of the trough width which is offset by just one MOLA footprint yields a difference of up to 400 m. However, our data are in good agreement with trough widths of up to 2 km, as suggested by *Morris and Underwood* [1978].

We determined the width for all the 169 investigated troughs from the MOLA profiles (Figure 6) and found that the width var-

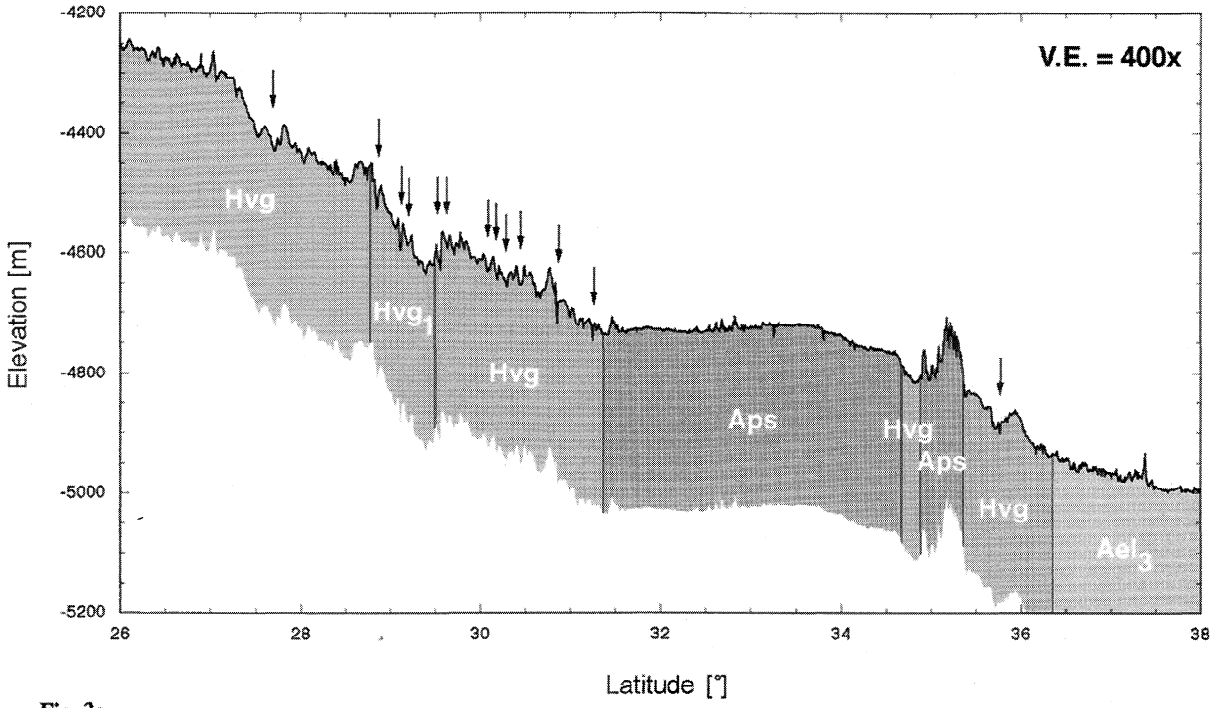

Fig. 3e

Figure 3. (continued)

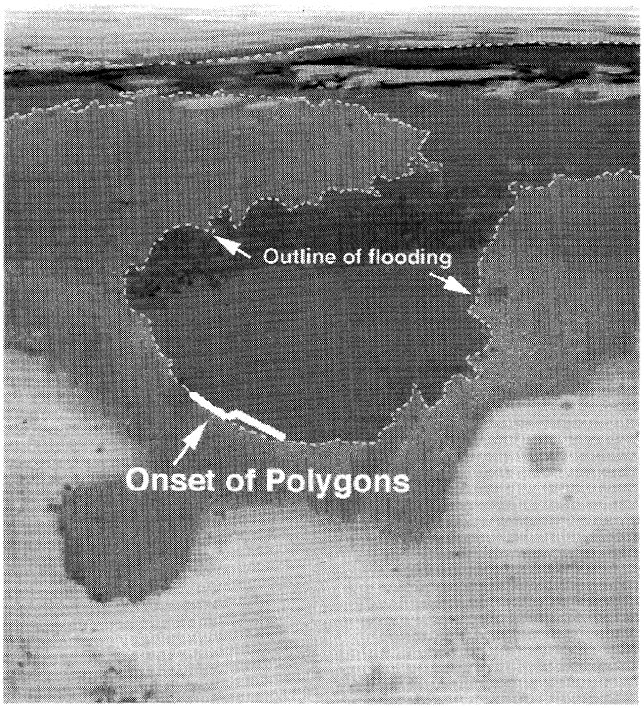

Figure 4. MOLA topography with superposed Viking mosaic. The Utopia basin was flooded to -4350 m (dashed line), the elevation of a terrace identified by *Thomson and Head* [1999]. Solid white line shows the location of the first polygon identified in the Viking and the MOLA data. Note that the first polygonal troughs occur near and below the location of the terrace and that the onset of the polygonal terrain closely follows the MOLA contour line, that is, the flooding level. Image covers approximately 90°x75°.

ies between <0.5 and 7.5 km. About 36% of all fractures show a width of <1.5 km and 72% of all troughs exhibit a width of <2.5 km. About 17% of the investigated troughs are smaller than 1 km in width. The mean fracture width is about 2 km with a standard deviation of 1.14.

The depths derived from the MOLA profiles (Figure 7) are in excellent agreement with the previously published data [*Pechmann*, 1980] and vary between <5 and 115 m. The mean depth of the investigated troughs is 32 m with a standard deviation of 22. The distribution of depths is asymmetric toward smaller depths and shows a broad maximum at depths smaller than 30 m; 62% of all measured troughs are shallower than 30 m. Although size and spacing of the MOLA footprint will cause underestimation of depth, our data suggest that depths of several hundred meters originally reported for polygons at 40°-50°N latitude by *Morris and Underwood* [1978] are overestimations.

We plotted depth and width of the polygonal troughs versus the distance from the basin center (45°N, 248°W) and found that the depth tends to increase toward the basin center (Figure 8). This means that some polygonal troughs appear to be deeper and more pronounced closer to the basin center. The width of the troughs is not as strongly correlated with the distance to the center as the depth. In our data we see faint hints that the width may slightly decrease toward the basin center, but further data are needed. As mentioned before, polygonal terrain in the center of the Utopia basin is covered by younger, Amazonian deposits of the Elysium Formation (Ael_3 in the geologic map of *Greeley and Guest* [1987]).

Dip angles of fractures forming polygon margins could provide important information on the processes of formation, but original dip angles have been modified by later processes such as aeolian infilling. Profiles oriented obliquely to the polygon

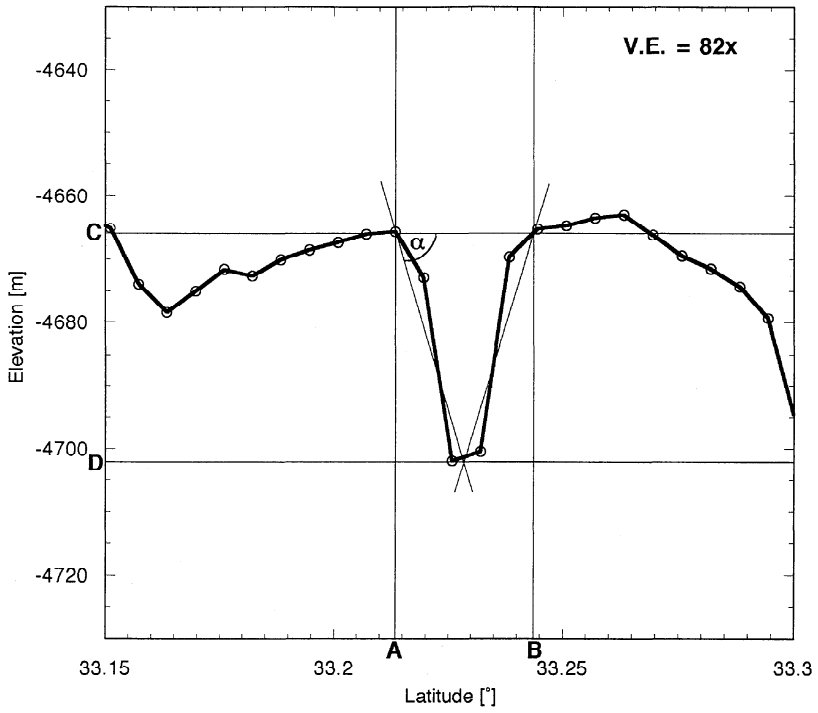

Figure 5. Profile across a typical polygonal trough that shows our approach to measure polygonal troughs. Width was measured between A and B, depth was measured between C and D, and α is the approximated slope angle.

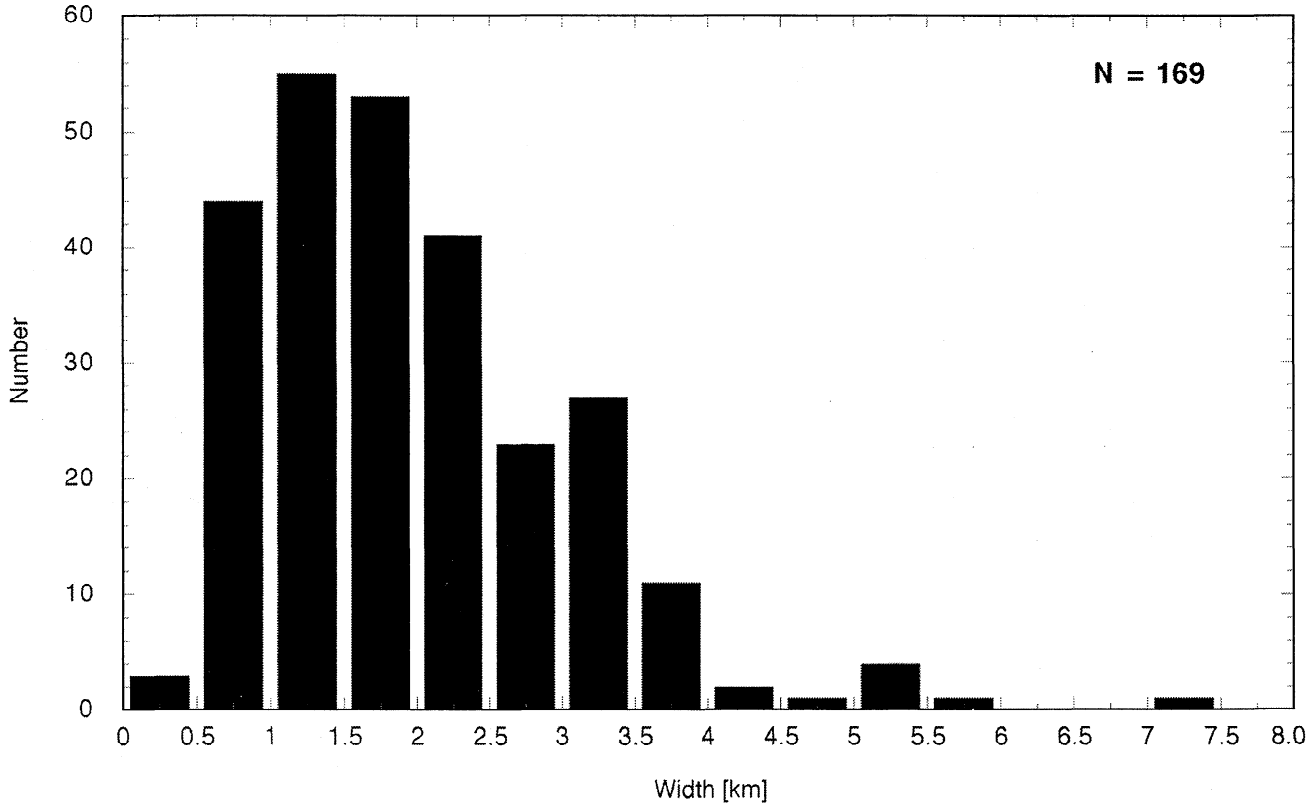

Figure 6. Histogram of 169 measured widths of polygonal troughs in southern Utopia Planitia. The mean trough width is about 2 km with a standard deviation of 1.14 km.

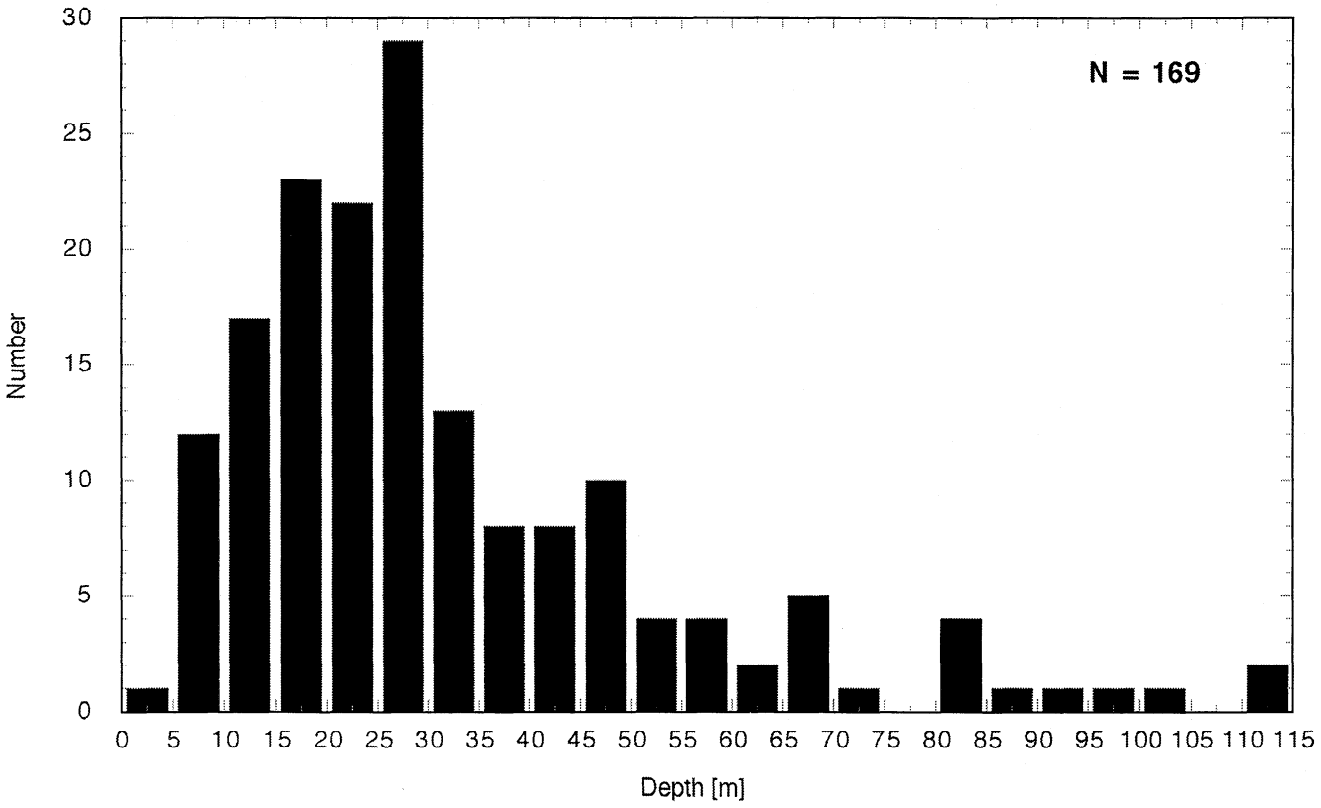

Figure 7. Histogram of 169 measured depths of polygonal troughs in southern Utopia Planitia. The mean trough depth is about 32 m with a standard deviation of 22.

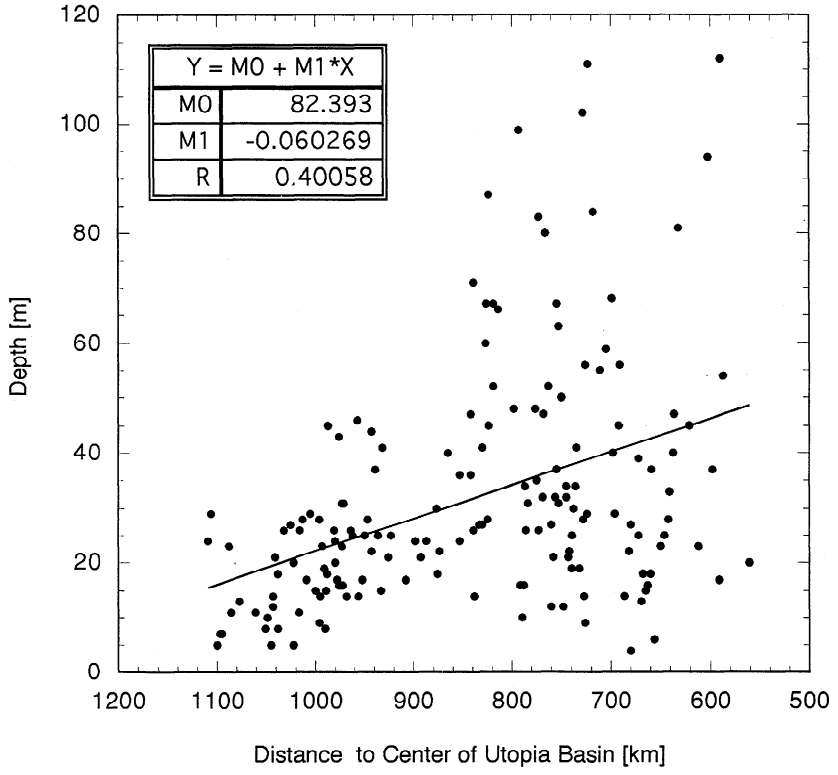

Figure 8. Depth of polygonal troughs in relation to the distance to the center of the Utopia basin. Deeper troughs appear preferentially closer to the basin center, whereas smaller and medium-size troughs are probably evenly distributed throughout the basin.

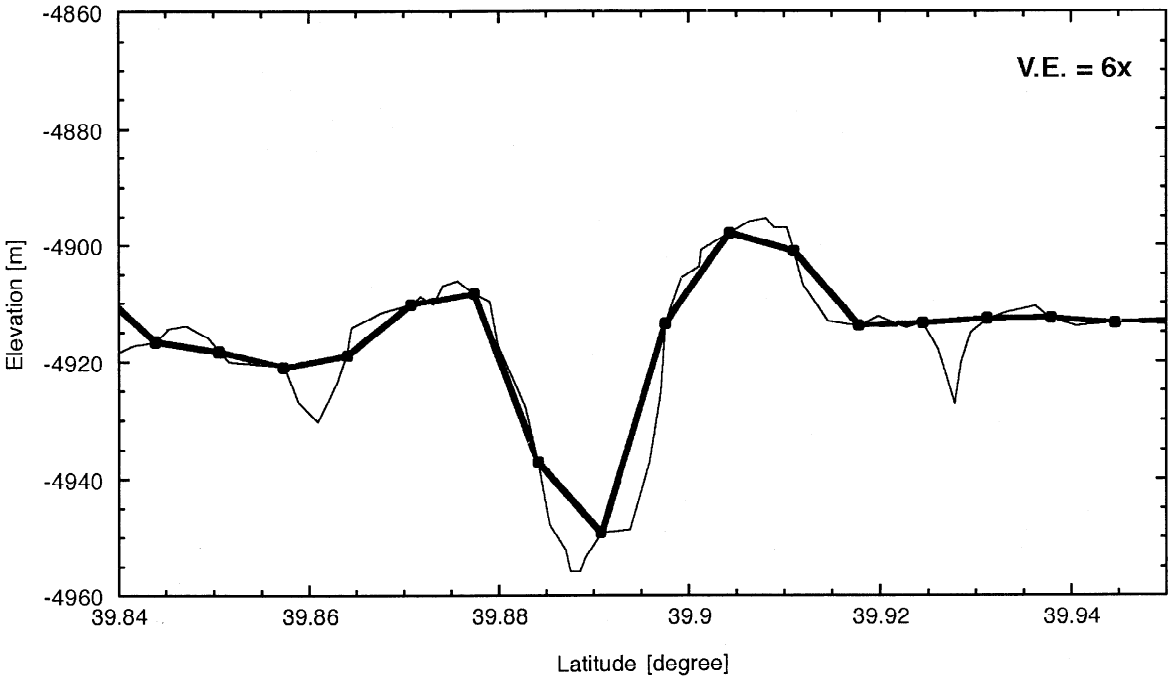

Figure 9. Schematic comparison of a hypothetical topography (thin black line) and its representation in the MOLA data (thick black line). Footprint size and spacing of MOLA points causes slope averaging and define the size of resolvable features in the profiles.

margins require correction to determine present slopes. We calculated slope angles based on the depth of a trough and the width, corrected for oblique cross cutting of the MOLA pass. Our slopes are estimates, as we do not know the exact morphology perpendicular to the trough orientation but only along the MOLA ground track. In addition, most of the troughs exhibit convex or rounded rims which yield systematically smaller slope angles if they were included in the measurements. At the base of the troughs concave debris aprons may have accumulated, also decreasing the dip angle. Footprint size and spacing of MOLA data points also causes slope averaging (Figure 9); using these data, slopes of trough walls are usually small with a mean slope of less than 3° and a variation from 0.5° to 15°.

3.4. Morphology

Investigating the morphology of individual troughs with MOLA, we see a broad variety ranging from simple v-shaped troughs to more complex u-shaped and w-shaped fractures. However, it should be kept in mind that small, simple v-shaped troughs might simply be the result of limited spatial resolution when the fracture is defined by only a small number of data points.

With this limitation in mind, we find that troughs may be symmetric or asymmetric in shape and can either show convex or concave walls. In our data we see that a large number of the troughs appear more or less symmetrical with convex shapes of the upper trough walls and concave shapes at the bottom. In the MOLA data some troughs show a morphology which could be interpreted as raised rims, but at Viking resolution (Figure 10) raised rims are rarely and in the spatially limited MOC images (e.g., Figure 11) raised rims so far are not observed. Raised rims in the MOLA profiles are in agreement with observations of *Helfenstein and Mouginis-Mark* [1980] on Viking images but in disagreement with observations by *Morris and Underwood* [1978] who noted that polygonal fractures are rounded and do not have rims or ramparts. *Ross and Kargel* [1998] observed raised rims of polygons in the close vicinity to the north polar ice cap, but these polygons are much more similar to the small-scale polygons we observed on the ejecta blankets of young fluidized crater than to giant polygons.

For the investigated area there are a number of MOC images available (39903, 41606, 41804, 41805, 43504, 43505, 47106, 47305, 47306, 49101, 52706) with resolutions varying from ~3 to ~10 m per pixel. Analysis of these images shows that polygonal troughs generally are broad graben-like features with variable morphologies. Most of the troughs exhibit parallel borders (i.e., a consistent width over several kilometers), but some also show an unequal widening in some parts of the trough (Figure 11). In the wider troughs, MOC images show morphologic features along the trough walls that can either be interpreted as terraces or as products of listric faulting. *Pechmann* [1980] interpreted terraces, visible in the Viking images, as products of normal faulting. In MOC image 39903 (Figure 11) we identified a chain of small circular depressions at the trough bottom which might be related to subsurface collapse or sublimation. A depression at the intersection between several troughs at the bottom edge of image 39903 may also be related to subsurface collapse. We also see evidence for numerous widened trough intersections in the Viking images (Figure 10). In MOC images, trough bottoms generally appear flat, and numerous troughs exhibit dunes indicating that the morphology of the original troughs was modified by later aeolian activity. We do not observe prominent raised rims on troughs in MOC images. Troughs can either be straight or undulating and narrower troughs appear straighter than wider ones but further data are required to investigate this

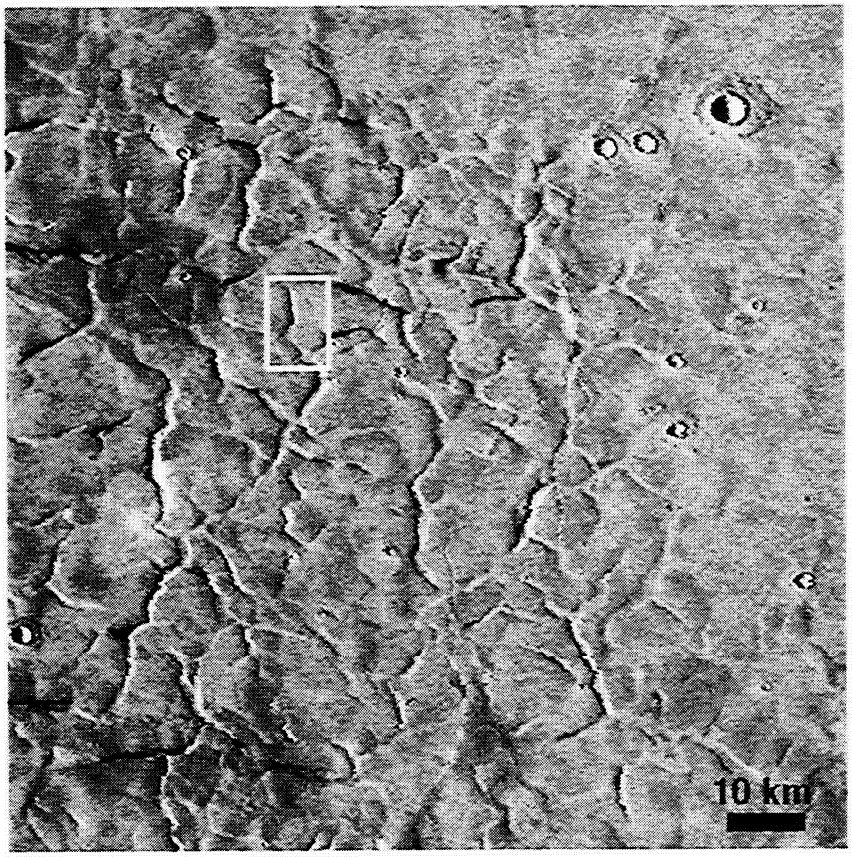

Figure 10. Viking mosaic with 230 m resolution of polygonal terrain in Utopia Planitia. White rectangle outlines the location (center at 33.46°latitude, 251.70°longitude) of MOC image 39903 shown in Figure 11. Note the broad graben-like appearance of the troughs, the wide variety in depths and widths, and that the troughs are narrower and shallower at their ends.

in more detail. We see a broad variety of trough widths, ranging from 100 to ~1800 m, but we do not see smaller polygonal patterns within the giant polygons. At MOC resolution the troughs are poorly interconnected, but some cross cutting of troughs is observable (Figure 11). The rarity of trough intersections observed in MOC data is consistent with the observations of *Pechmann* [1980] made in Viking images. Depth can vary along the trough. In some cases we see that a trough begins very shallow and becomes gradually deeper along its length. In other cases we observed that the deepest part is in the middle of the trough. We also observed very faint "ghost" troughs in several MOC images and it is unclear whether these troughs are old and filled or if they are young and at the beginning of their formation process.

In images 43505, 47305, and 47306, small-scale polygonal terrain is found on the fluidized ejecta blankets of impact craters (Figure 12). These troughs are much smaller than the troughs described above, are more strongly interconnected with each other, and frequently show hints of raised rims. For the small-scale polygons on the ejecta blankets we conclude that their formation is closely related to a volatile-rich substrate. Provided that craters with fluidized ejecta form in volatile-rich substrates [e.g., *Mouginis-Mark,* 1979, 1981, 1986; *Kuzmin et al.,* 1988a, b; *Squyres et al.,* 1992; *Cave,* 1993; *Barlow,* 1994; *Costard and Kargel,* 1995], these polygons might have formed when a warm, wet ejecta blanket cooled and desiccated.

3.5. Strain Values

Polygonal troughs were used [*Pechmann,* 1980] in order to calculate the extensional strain that acted to form polygonal terrain. This is only possible under the assumption that the polygonal troughs represent simple tension cracks and were not widened by erosional processes. However, the morphology of the troughs as seen in the MOLA profiles and MOC images indicates a modification of the original trough morphology. MOC images (e.g., 41804, Figure 13) show the troughs to be broad, shallow, graben-like features with rounded rims. Some troughs exhibit a sharp morphology, but we also find evidence for subdued trough morphology. The MOC images also show sand dunes on the floor of the troughs (Figures 11 and 13); clear evidence for aeolian modification of the trough. From these observations we conclude that an erosional widening of the trough morphology is likely to be common and must be taken into account when calculating strain. Results derived from data of the Mars Orbiter Laser Altimeter (MOLA), the Mars Orbiter Camera (MOC), and the Viking Orbiter for the investigation of polygonal terrain are summarized in Table 1.

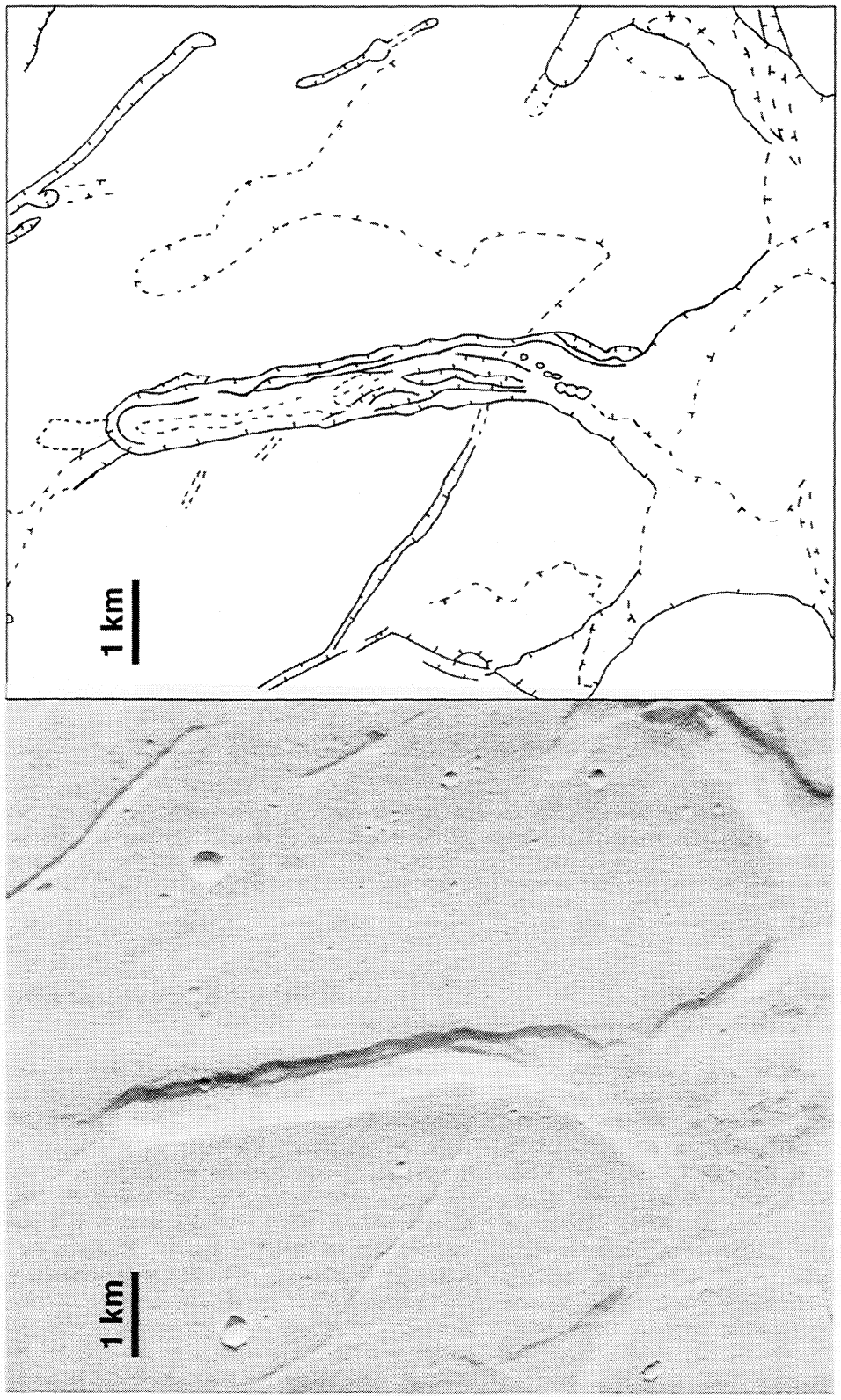

Figure 11. MOC image 39903 (4.06 m spatial resolution; 33.46°latitude, 251.7°longitude) and sketch map of the area. Polygonal troughs appear as graben-like flat-floored features. Rims are sharp (but not obviously raised) and terraces are visible. At the lower right image corner a small trough seems to cross cut a wider trough. Aeolian deposits (dunes) can be observed at the trough bottoms. Also visible is a very subdued trough-like depression right of the image center and a wide depression at the image bottom where several troughs intersect.

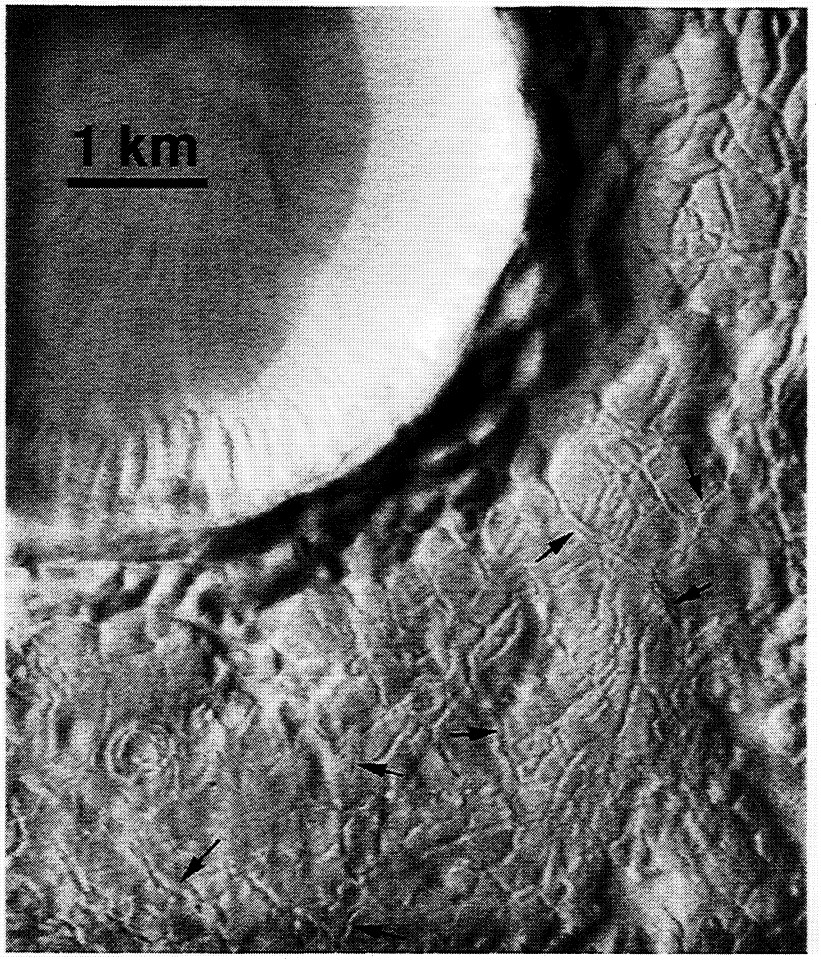

Figure 12. MOC image 47306 (6.74 m spatial resolution; 32.9°latitude, 243.98°longitude) showing small-scale polygonal terrain on the fluidized ejecta blanket of an impact crater. These small-scale polygons were formed by different processes than the giant polygons and therefore show different characteristics. Desiccation and/or thermal contraction of a volatile-rich ejecta blanket most likely have formed these polygons. Black arrows point to troughs with raised rims. Streaks on the crater floor and scouring of the inner crater wall may indicate erosion by water.

4. Review of Models for the Formation of Polygonal Terrain and Outstanding Questions

Numerous models have been proposed to explain the origin of Martian polygonal terrain. All of these models generally involve cracking in response to tension. An important unsolved question is whether the material of the polygonal terrain is of sedimentary [e.g., *McGill*, 1986, 1987; *McGill and Hills*, 1992; *Lucchitta et al.*, 1986] or of volcanic origin [e.g., *Masursky and Grabill*, 1976; *Carr et al.*, 1976; *Morris and Underwood*, 1978; *McGill*, 1986, 1987]. The models interpret the troughs which form the large-scale polygons as resulting from loading of sediments with volatile-rich lavas [*Helfenstein and Mouginis-Mark*, 1980], cooling of lava flows [e.g., *Masursky and Grabill*, 1976; *Carr et al.*, 1976; *Morris and Underwood*, 1978], coalescence of smaller polygons [*Helfenstein and Mouginis-Mark*, 1980], tectonic processes [*Mutch et al.*, 1976], tectonic bending over a rough subsurface [*McGill and Hills*, 1992], convection within a wet sediment layer [*Wenrich and Christensen*, 1993, 1996], thermal contraction [*Carr and Schaber*, 1977], and desiccation of wet sediments [*Morris and Underwood*, 1978].

4.1. Basalt Loading Onto Water-Saturated Sandstone

Needham [1978] described the formation of circular and rectilinear structures in northern Australia as due to density instabilities which are caused by a denser basalt overlying a less dense wet sandstone. The basalt layer produces an excess of hydrostatic pressure over lithostatic pressure, which led to a rheological deformation of the soft sediments. *Helfenstein and Mouginis-Mark* [1980] cited this process as a possibility for the formation of Martian polygons. However, the scale of the Australian structures is up to 250 m in diameter; smaller than the Martian features by at least a factor of 10. Also, the Australian polygonal structures are depressions, which are encircled by ridges up to 10 m in height, whereas Martian polygons are bounded by troughs, which can be identified in the Viking images. To make the polygonal structures visible, the basalt has to be eroded (Figure 14a). Could such a process have formed the polygons in Utopia? *McGill and Hills* [1992] report that polygonal terrain in Utopia Planitia can be circumscribed by a circle with 17° (~1000 km) radius, equivalent to a surface area of 3.2×10^6 km^2. Today about 1/3 of this area is

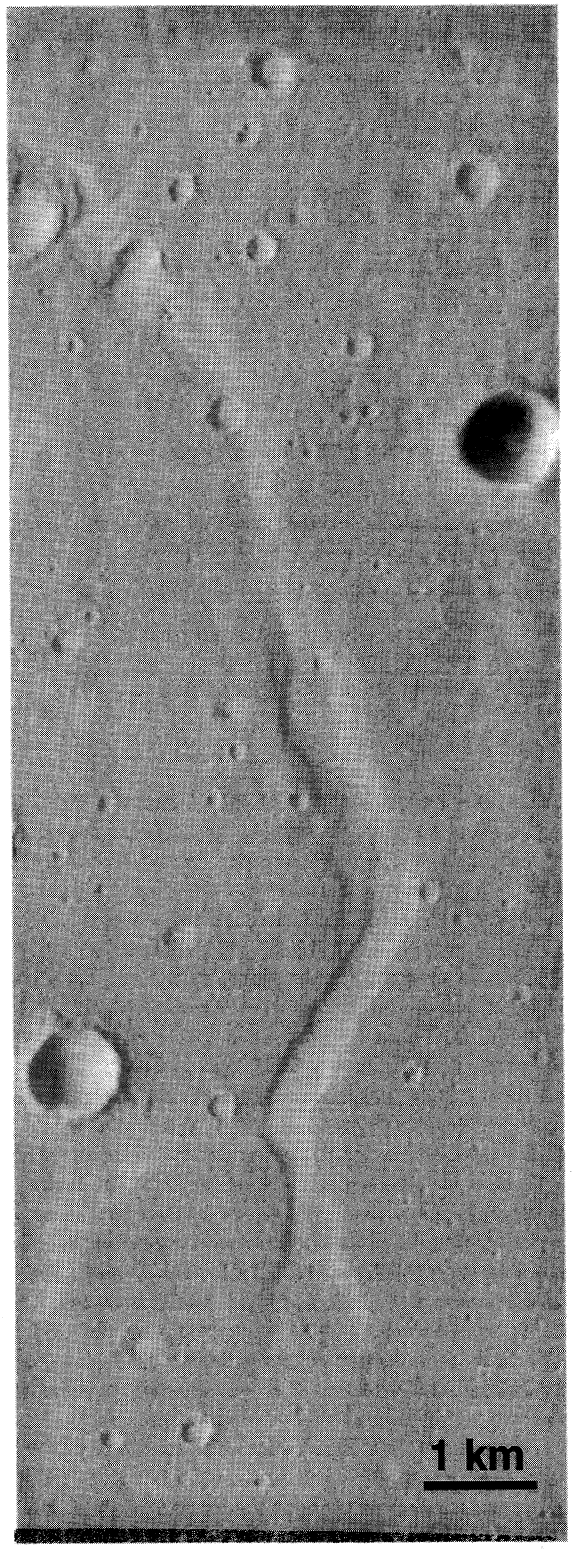

Figure 13. MOC image 41804 with 4.78 m spatial resolution (30.41°latitude, 245.74°longitude). Morphology of polygonal troughs is modified by aeolian deposits, that is, dunes. Some rims are sharp, others are rounded and subdued. Northern end of the trough appears to be narrower and shallower than the middle parts. These observations are similar to observations of troughs in the Caloris basin on Mercury for which a tectonic origin was proposed [*Strom et al.,* 1975].

covered with polygonal terrain but according *to McGill and Hills* [1992] it is highly likely that polygonal terrain is also located beneath the Amazonian deposit (Ael_3) which was interpreted by *Christiansen* [1989] to be a lahar stream from Elysium Mons. Widespread erosion of basalts, which according to the model must have originally covered the polygonal terrain over such a large area, is unrealistic, especially as we do not see the deposition of the eroded material elsewhere in the enclosed Utopia basin.

4.2. Cooling of Volcanic Material

Martian polygonal fractures were also attributed to cooling of lava [*Masursky and Grabill*, 1976; *Morris and Underwood*, 1978]. *McGill and Hills* [1992] conclude from their observations of superposition relationships between craters and troughs and from probable material elastic and quasi-viscous properties that the formation of polygonal troughs was a rapid geologic process that occurred "immediately" after the deposition of the polygonal terrain material. *Pechmann* [1980] pointed out that in the case of a cooling lava flow the surface should be saturated with small fractures, no matter how slow the cooling rate of the lava is (Figure 14b). Experiments by *Müller* [1998] indicate that the column diameter is controlled by the temperature gradient at the crack front and not by the cooling rate of the lava flow. According to *Müller* [1998], a low-temperature gradient at the crack front and high diffusivity produce thicker columns, that is, wider polygons. As no similar sized patterns exist on terrestrial or lunar volcanic provinces, *Pechmann* [1980] concludes that this formation process seems unlikely.

Large-scale polygons, similar in size to Martian polygons, are known from Venusian lava flows [*Johnson and Sandwell*, 1992], but these are restricted to very limited areas near coronae. Polygons southeast of Nightingale Corona (Magellan image F-MIDR.60N132) are typically of the order of 1-8 km with larger polygons closer to the corona structure. The widths of the polygonal troughs vary from 75 m (image resolution) at the southern portion of the image to 500 m close to Nightingale Corona. *Johnson and Sandwell* [1992] exclude a formation due to regional stress fields because the polygonal pattern is isotropic. They favor a formation analogous to joint networks found in terrestrial lava flows. However, the limited occurrence of polygonal terrain on Venus, the close vicinity to coronae structures, and the different size of polygons in relation to the distance to the corona are consistent with structural uplift and rather suggest a tectonic formation. We consider tectonic uplift as a possible process for the formation of giant polygons not only on Venus but also on Mercury and Mars.

4.3. Tectonic Deformation

Phase changes in rocks of the interior can result in an increase of the Martian radius of approximately 10-20 km corresponding to a linear expansion of 0.3-0.6% at the surface and lead to extensional tectonism (Figure 14c) which could have formed polygonal terrain [*Mutch et al.*, 1976]. However, no known tectonic structure of any scale on Earth is similar in morphologic detail to the Martian polygonal pattern [*McGill*, 1986; *Pechmann*, 1980]. *Morris and Underwood* [1978] argued that a regional tectonic stress field would yield a more regular

Table 1. Summary of Observations and Results Obtained From the Investigation of MOLA, MOC, and Viking Data

Characteristics	Observations
	MOLA
Location (Plate 1, Figure 4)	occur within the Utopia Basin
Elevation (Figure 3)	wide range of elevations; lower parts of basin structure
Slopes (Figure 3)	exposed on gentle slopes of ~0.1°
Onset (Figures 3 and 4)	close to the same elevation in several profiles; close to the same elevation of a terrace, interpreted to be a shoreline of a former standing body of water
Depth (Figures 7 and 8)	range from <5 to 115 m; average is about 30 m; increases toward the basin center
Width (Figure 6)	mean width is about 2 km
	MOC
Morphology (Figures 11-13)	generally broad, graben-like; terraces may or may not occur; variations in lobateness, depth, and width; circular depressions at the bottoms observed for some troughs
Modifications (Figures 11 and 13)	numerous dunes are evidence for aeolian modification processes
Interconnections	troughs are weakly interconnected
Troughs on ejecta blankets (Figure 12)	polygonal troughs on ejecta blankets of young craters with fluidized ejecta blankets show different morphologies than giant polygons, for example, raised rims; smaller in size; more heavily interconnected
	VIKING
Crater Morphology (Figures 1 and 2)	large number of crater with fluidized ejecta blankets (ramparts, single and double lobes) superposed on polygonal terrain
Depth of crater burial (Figure 2)	old impact craters increasingly buried toward the basin center

geometry than that displayed by the polygons. However, a tectonic origin could explain the preferred trough orientations in some regions, circular troughs, associated ridges and domes, and most important, the large scale of the polygons [*Pechmann*, 1980]. Besides the increase of the planetary radius, there are two other possibilities to produce extensional tectonics in the Martian crust; nonuniform horizontal movement and updoming. So far, large-scale horizontal movements have not been observed on Mars, and evidence suggesting plate tectonics [*Sleep*, 1993] is not uniformly accepted [*Carr*, 1996]. *Beloussov* [1962] reports experiments of Y. I. Chertkova that have shown that circular uplift and downwarping are accompanied by radial and concentric fractures which produce a "turtle structure" similar to polygonal terrain. However, the fracture pattern may vary significantly if the uplift is not round but elongated. Updoming is a possible theory for the origin of giant Martian polygons because of the preferred trough orientations and the similarity to radial and concentric troughs in the Caloris basin on Mercury [*Pechmann*, 1980]. According to *Pechmann* [1980], polygonal fractures on Mars represent graben which where formed in response to a nearly isotropic, horizontal tensional stress. Local uplift which imposed such an isotropic, horizontal extensional stress field and allowed the formation of a complex deformation pattern, was also proposed for the Noctis Labyrinthus region [*Tanaka and Davis*, 1988]. Morphologically, the troughs in the Caloris basin show the same tendency to shallow and narrow at the ends as was observed for Martian troughs in the Viking images [*Pechmann*, 1980] (Figure 10). *Strom et al.* [1975] mention that the length and the width of the fractures at the Caloris floor increase toward the basin center. The fractures range in width from about 700 m (image resolution) to 7-9 km; the wider fractures appear to be flat-floored and graben-like with depth of the order of 300 m [*Strom et al.*, 1975]. The Caloris floor shows a dominant concentric tensional fracturing and a weaker radial trend. Concentric and radial fracture patterns are consistent with either uplift or subsidence. As the fractures at the Caloris floor are associated with probably older ridges, *Strom et al.* [1975] proposed that the floor subsided causing concentric and radial stresses to form the ridges. Following subsidence, a possible uplift finally produced crustal lengthening and the observed fracture pattern. *Cartwright and Dewhurst* [1998] report on polygonally oriented fault systems associated with 27 marine basin structures on Earth. New three-dimensional (3-D) seismic studies of Tertiary mudrocks in the North Sea show extensional faults which are organized in polygonal networks with greater or lesser degrees of connectivity [*Cartwright and Lonergan*, 1996; *Lonergan et al.*, 1998; *Lonergan and Cartwright*, 1999]. The faults are randomly oriented, have dip angles of about 45° and a spacing of up to 1 km. The faults have throws varying from 10 to 100 m and are interpreted to have formed by volumetric contraction during compactional dewatering in response of shallow burial [*Cartwright and Lonergan*, 1996; *Lonergan et al.*, 1998; *Lonergan and Cartwright*, 1999]. *Cartwright and Dewhurst* [1998] suggested a model of formation of these compaction-related faults due to syneresis whereby pore fluid is expelled from sedimentary gels under the spontaneous action of osmotic or electrochemical forces. On Earth, polygonal faults only occur in fine-grained (<2 mm) sediments with high-porosity, low-permeability, and high specific surface area. Polygonal faults are restricted to two lithologies, clays and claystones, and oozes and chalks [*Cartwright and Dewhurst*, 1998]. Sedimentary processes within Martian ocean basins could have formed some of these rock types.

4.4. Coalescence of Smaller Polygons

Based on their investigation of polygonal terrain in Utopia Planitia, Acidalia Planitia, and the polar regions, *Helfenstein and Mouginis-Mark* [1980] concluded that regional differences in polygon size reflect material effects such as volatile con-

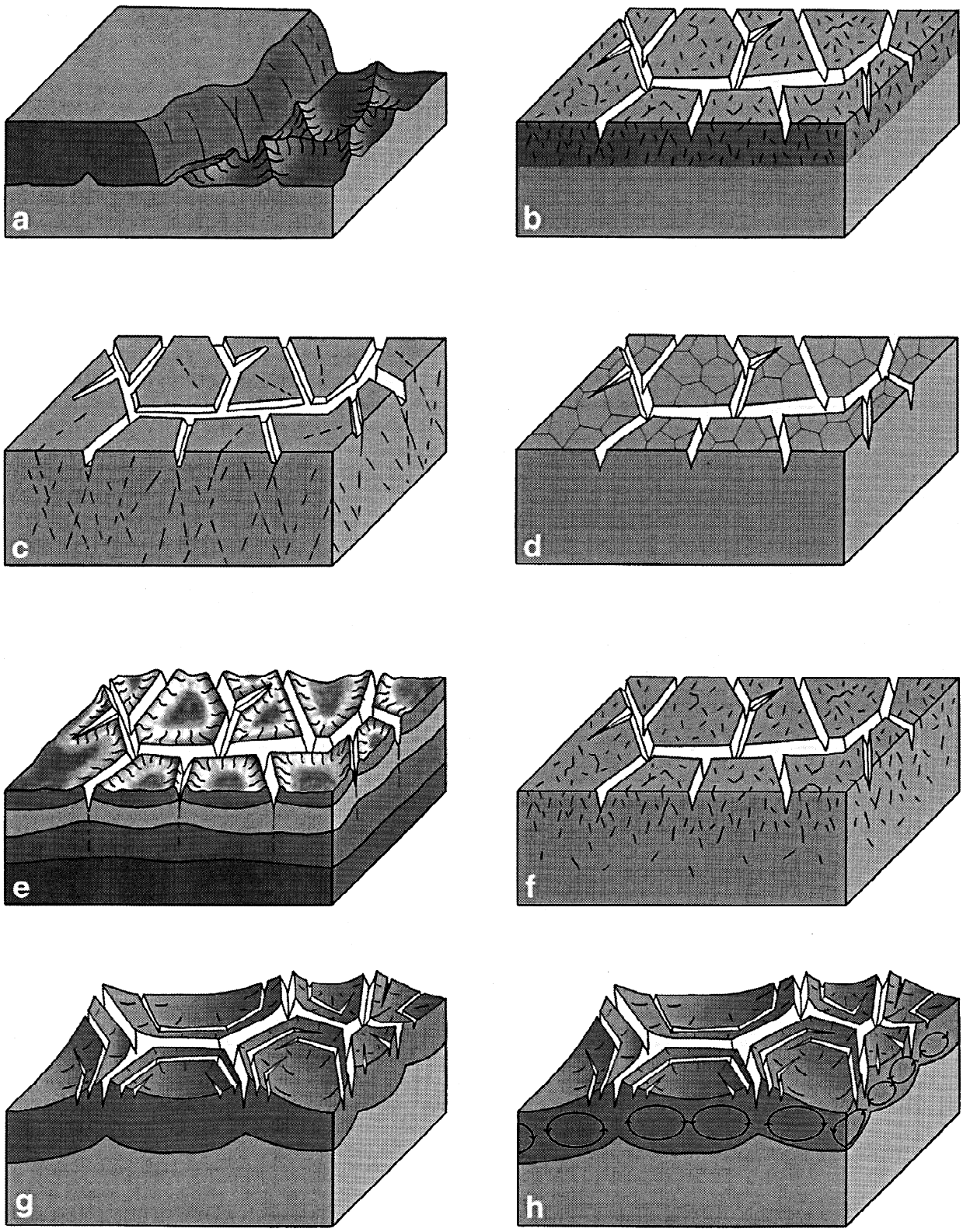

Figure 14. Block diagrams to illustrate the models for the formation of polygonal terrain: (a) basalt loading (b) cooling of a basalt flow, (c) desiccation, (d) thermal contraction, (e) bending over a rough subsurface, (f) convection, (g) coalescence of smaller polygons, and (h) tectonic origin. See text for discussion.

tent, particle size, or the degree of lithification. Similar morphologies (e.g., raised rims, comparable intersection angles) let them to the conclusion that Martian polygons are analogs to terrestrial ice-wedge polygons (discussed below under thermal contraction). However, the large size of Martian polygons is a major objection to a number of models, such as the desiccation and thermal contraction models. Their observation that the troughs of larger polygons are often curved or slightly meandering and tend to follow 120° intersection angles of smaller polygons led *Helfenstein and Mouginis-Mark* [1980] to introduce a "gravity scaling" parameter which takes into account the lower lithostatic stresses on Mars. According to their theory, initially only Martian polygons 2 to 3 times the size of terrestrial analogs have to be formed by ice wedging. Larger polygons would then form by coalescence of these smaller polygons (Figure 14d). In order to do this, *Helfenstein and Mouginis-Mark* [1980] proposed that a desiccation process might have operated to enlarge the polygons. However, meandering troughs do not prove coalescence of smaller polygons and may simply be the result of crack development and en echelon (i.e., overlapping) propagation as described by *Beloussov* [1962] and *Johnson and Sandwell* [1992]. In addition, *Pechmann* [1980] noted that the local preferred trough orientation and the flat-floored, steep-sided cross sections are difficult to explain by a formation due to ice wedging. From Earth we have evidence from the playas of the Great Basin that smaller polygons can occur within giant polygons [*Neal et al.,* 1968]. However, these desiccation polygons are shallow surface mud cracks with ~30 cm diameter that occur in large polygons of 15-300 m diameter [*Neal et al.,* 1968]. Figure 1 of *Neal et al.* [1968] shows the relation between the small polygons, and a fracture that outlines a giant polygon and in our opinion there is no evidence that the large fracture followed the outlines of the small polygons but rather formed at the expense of smaller polygons.

4.5. Desiccation

Large-scale terrestrial polygons formed by desiccation (Figure 14e) range in diameter from 15 to 300 m and show fractures a few centimeters to 1 m in width and up to 5 m and more in depth [*Neal et al.,* 1968]. At intersections of terrestrial desiccation fractures a widened collapse hole is often noticed [*Neal et al.,* 1968] and a wide depression at the intersection of several Martian troughs (bottom of Figure 11; Figure 10) can probably be interpreted as such a collapse feature. In addition, we see a pitted texture at the bottom of the trough in Figure 11 which could be related to subsurface collapse or sublimation of ground ice. Mud cracks have been thought of as downward propagating cracks that nucleate at the surface and terminate at depth [*Neal et al.,* 1968], because the rate of moisture loss and capillary forces decrease downwards, as do tensile stresses. The depth of the cracks and their spacing are therefore determined by the depth of the water table because most cracks do not propagate through the zone of saturation [*Pechmann,* 1980]. Alternatively, a crack can propagate downward to a level where horizontal stress becomes compressive as a result of the weight of overlying sediments [*Allen,* 1985].

However, new results of *Weinberger* [1999] for stratified sediments indicate that nucleation at depth and upward propagation of cracks is a far more common mechanism than previously thought. Weinberger's results show that the cracks originate at very small dimples or fine holes and are occasionally associated with relatively coarse grains. As polygonal terrain is not restricted to Earth but can also be located on other planets like Mars, the striking similarity of Martian polygons to terrestrial mud cracks led to the interpretation that the Martian polygons were formed by shrinkage related to desiccation of water- or ice-rich sediments [*Morris and Underwood,* 1978]. However, as polygons on Mars are at least an order of magnitude larger than terrestrial polygons, *McGill* [1986] concluded that terrestrial polygons are not a valid mechanical analog for the formation of the Martian polygons. *Pechmann* [1980] also sees a serious scaling problem: even under the lower gravity of Mars, vertical cuts produced by tension cracks could only be stable to 15-20 m depth because deeper cracks would collapse due to the overburden pressure and the tendency of soils to creep. *Pechmann* [1980] notes that this is in disagreement with the observation that the fractures can be up to >100 m deep [*Morris and Underwood,* 1978]. *Lucchitta* [1983] argues that the equatorial regions are most desiccated because water is in disequilibrium with the atmosphere and would consequently sublime from the ground. Therefore giant polygons would preferentially form near the equator between ±40° latitude. *Lucchitta* [1983] argues that this is not consistent with observations on Viking images. For the northern polygonal terrain, *Lucchitta* [1983] suggests that during astronomic cycles of 10^5-10^6 years the high latitudes could have been warmed sufficiently to form polygons. She concludes that desiccation due to climatic cycles can initiate the formation of small-scale polygonal terrain near the polar regions and that secular desiccation is not a likely process for the origin of polygonal terrain at lower latitudes.

4.6. Thermal Contraction

Terrestrial polygons in permafrost environments are formed by deep thermal contraction cracking of frozen soil (Figure 14f) and a subsequent widening of the cracks [*Higgins et al.,* 1990]. This widening occurs over many perennial cycles by repeated cracking of the ice-rich ground. Frost accumulates in the fracture which, reopening at times of low temperature, acquires more frost, and so the ice wedge is gradually widened [*Flint,* 1971]. Because the growth of an ice wedge implies its existence without thawing for hundreds or even thousands of years on Earth, ice wedges indicate the presence of permafrost [*Flint,* 1971]. Terrestrial polygons formed by thermal contraction are 5 to 30 m in diameter and the cracks are as much as 7 or 8 m deep [*Higgins et al.,* 1990]. Despite the large differences in size between Martian and terrestrial polygons, a formation of Martian polygons by thermal contraction was originally proposed by *Carr and Schaber* [1977]. According to *Lucchitta* [1983], seasonal temperature changes of about 60°C at latitudes of 45°N are sufficient to initiate thermal contraction in ice-rich ground. *Lucchitta* [1983] argues that the thermal contraction hypothesis is consistent with theoretical and observational evidence for ground ice.

Black [1978] rejected the thermal contraction theory and argued that the size of the giant polygons is incompatible with terrestrial thermal contraction processes. For an expected temperature range between -50°C and -110°C the coefficient of linear expansion for ice is 4×10^{-5}/°C and 3×10^{-5}/°C, respectively [*Hobbs,* 1974]. Taking these numbers from *Lucchitta* [1983], the thermal contraction for 50-300 m wide polygons would be of the order of 9-72 cm. Therefore the cracks would not be visible at 11 m/pixel resolution of the Viking images 458B67

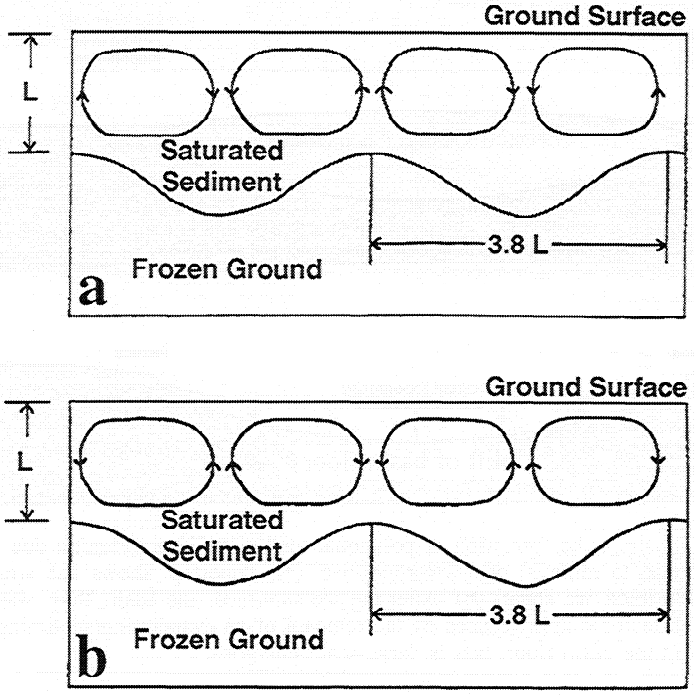

Figure 15. Two versions of a schematic cross section of hexagonal Rayleigh convection cells from *Wenrich and Christensen* [1993, 1996]. See text for discussion.

and 458B69 which were the basis for Lucchitta's observations. For a 10 km wide polygon and a temperature drop of 100°C, *Pechmann* [1980] calculated a maximum possible crack width of 50 m, and he concluded that any model that forms polygonal troughs by thermal contraction must include a mechanism to widen the cracks. Such a widening can be produced by repeated thermal cracking followed by infilling with sediment or frost. In the dry, Martian climate the fractures may be filled by material blown into the fractures to form sand wedges but disintegration of the ground along polygonal terrain also favors the formation of ice wedges [*Lucchitta*, 1983].

From terrestrial observations we know that the largest and best developed terrestrial ice wedge polygons are located on elevated, relatively well-drained and coarse outwash from glaciers [*Corte*, 1963]. Based on results of viscoelastic modeling of permafrost [*Lachenbruch*, 1962] and field observations in the Arctic, *Pechmann* [1980] pointed out that thermal contraction is confined to the upper 10 m of a surface layer and that the rapid temperature changes at depth which are required to form deep fractures are unlikely. Results from *Lachenbruch* [1962] indicate that for the formation of thermal contraction cracks the rate of temperature drop is far more important than the actual magnitude of the temperature drop. At slow rates, large stresses relax quickly due to creep within the ice [*Pechmann*, 1980]. Therefore thermal contraction is essentially a near-surface phenomenon and would not be able to produce deep fractures because the temperature changes are too small at depth.

4.7. Tectonic Bending Over a Rough Subsurface

A more recent concept for the formation of the giant polygonal terrain was proposed by *McGill* [1986] and *McGill and Hills* [1992]. Superposition relations and crater ages suggest that the formation of the polygonal fractures is closely related in time to the deposition of sedimentary or volcanic material rather than to later tectonic or periglacial processes [*McGill and Hills*, 1992]. From terrestrial studies it is known that fine-grained pyroclastics or wet sediments not only shrink with cooling or drying but also compact. Assuming a rough buried topography, *McGill and Hills* [1992] suggested that differential compaction will cause bending of the compacting layers over topographic highs such as crater rims (Figure 14g). The proposed process will superpose additional tensile stress onto horizontally isotropic tensile stresses produced by shrinkage. The tensile stress, which results from a combination of compaction and shrinkage, will be largest over topographic highs and therefore fractures will preferentially occur at these locations. The advantage of this model is that the size of the polygons can be attributed to the scale of the buried subsurface and is therefore completely independent of the fracturing process itself. The major implication of *McGill and Hills*' [1992] model for polygon formation is that fractures should preferentially occur over local topographic highs because stress is largest in those areas.

4.8. Density-Driven Free Convection

This model [*Wenrich and Christensen*, 1993, 1996] suggests that an undulatory subsurface produced by differential melting controls the polygon size (Figure 14h). The model presented in 1993 was a qualitative discussion of how a terrestrial convection model could be applied to Mars. In the work by *Wenrich and Christensen* [1993] a water/sediment is deposited by the outflow channels on top of the frozen lowland sediments. The denser, warmer surface water sinks and displaces colder less dense water to the surface (Figure 15a). This can happen because water at 277 K is 0.0132% denser than at 273 K. According to *Wenrich and Christensen* [1993], numerous convection cells are formed, and melting of the permafrost is enhanced beneath the downwelling warmer water relative to the

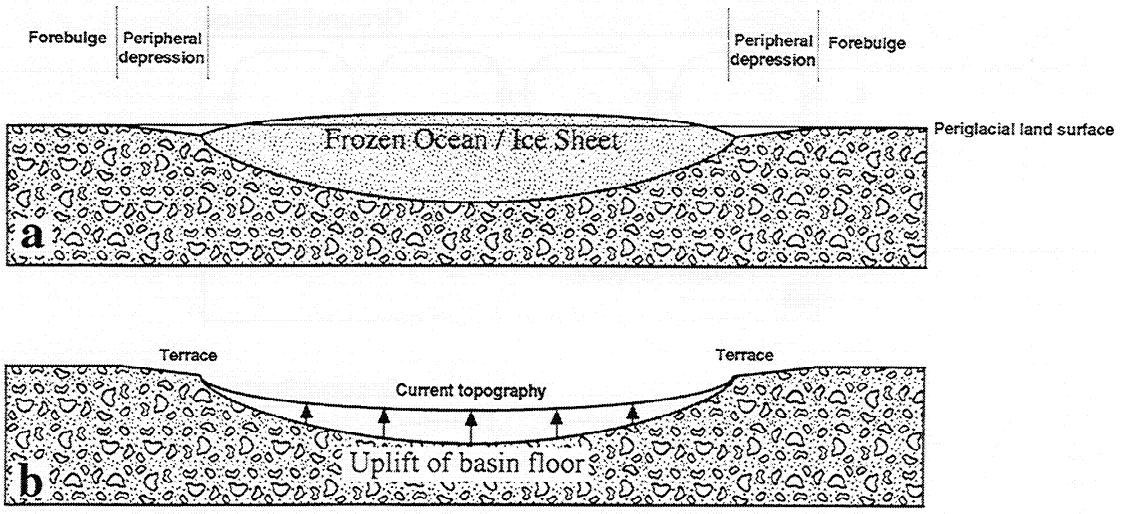

Figure 16. Sketch to illustrate the formation of polygonal terrain in Utopia Planitia due to tectonic uplift of the basin floor in response to removal of a water/ice load. (a) Timestep shows the situation when Utopia Planitia is covered with a thick ice sheet. (b) After the ice sublimed, the basin floor was uplifted to today's elevation. In this model, tectonic uplift caused by the removal of an evaporating/subliming ocean or ice sheet would lead to fractures in the basin floor, that is, large-scale polygons.

area beneath the cooler upwelling water. This differential melting causes a scalloped texture on the permafrost subsurface that later defines the size of the polygons.

In more recent work, *Wenrich and Christensen* [1996] adapted the terrestrial model to actual Martian conditions. In this scenario a water/sediment mixture starts cooling from the upper surface of the deposit due to the existing cold climate. When the temperature of the surficial pore water reaches 277 K, cooler than the underlying water, unstable density stratification occurs because water at 277 K is densest. This causes the cooler water to sink down (Figure 15b). The cooler water displaces the warmer underlying water, and melting of the permafrost is inhibited beneath the downwelling cooler water compared to the area of upwelling warmer water. Again, this differential melting creates an undulatory subsurface permafrost layer whose peak spacing is related to the size of the convection cell and also controls the size of the polygons. In both model varieties the water/sediment layer undergoes compaction due to desiccation and bending stresses due to gravity. Desiccation causes the soil to shrink and fracture uniformly, but the greatest tensile stresses occur above the formed subsurface topographic highs, similar to the model of *McGill* [1986] and *McGill and Hills* [1992]. For polygons of 5-20 km size, both model varieties predict a thickness of the outflow sediments of 1.31-5.25 km. The predictions of the sediment thickness of 1.31-5.25 km are not consistent with observations of *McGill* [1987] and *McGill and Hills* [1992] who estimated the thickness to be of the order of 500-600 m.

5. Discussion of Implications of MOLA and MOC Data and Testing of Hypotheses

Fundamental questions concerning giant polygonal terrain are the kind of environment in which it formed and the process responsible for its formation. With MOLA and MOC data we can not only investigate the geometry and the morphology in detail but also study the topographic position of polygonal terrain in a wide areal context. As a result (also see Table 1), we see that (1) polygonal terrain in Utopia Planitia is located on the lower slopes of the Utopia basin proper, (2) the onset of polygonal troughs in the investigated profiles is close to the same elevation and that of a distinctive terrace, (3) polygonal terrain in southern Utopia Planitia does not occur at a single topographic level but is located over a wide range of elevation on gentle slopes of ~0.1°, (4) the depths of polygonal troughs range from <5 to 115 m, averaging about 30 m, and increase toward the basin center, and (5) the average trough width is about 2 km. Data from the Mars Orbiter Camera (MOC) indicate that (1) the troughs are generally broad graben-like features with varying morphologies (i.e., occurrence of terraces, lobateness, widths, depths), (2) the morphology of the troughs was modified by aeolian processes, (3) polygonal troughs are poorly interconnected at MOC resolutions and there are no smaller polygons observed within the giant polygons, (4) circular depressions can occur at the bottoms of polygonal troughs, (5) polygonal terrain on the ejecta blankets of young craters with fluidized ejecta in this area exhibits different characteristics (i.e., size, rims, and degree of interconnections) than giant polygons. In addition, based on Viking images we see that (1) old impact craters are increasingly buried with younger material toward the basin center and that (2) superposed impact craters on polygonal terrain exhibit distinctive ejecta morphologies such as rampart ejecta blankets and single and double lobate ejecta blankets.

What are the implications of the new MOLA and MOC results for the formation processes? As we can not distinguish between volcanic and sedimentary material in the MOLA data, it is not possible to directly address the question of the origin of the substrate on which polygonal terrain formed. MOC images also show no unambiguous evidence for either volcanic or sedimentary origin of the polygonal terrain. However, the location of large-scale polygonal terrain on the slopes around a basin structure, the onset at about the same elevation in all investigated profiles and the relationship to a terrace interpreted to have formed by water [*Thomson and Head*, 1999] rather ar-

gues for formation in association with sediments. In addition, we do not see features suggestive of volcanic flow fronts in the Viking and MOC images and in the MOLA data. Finally, we do not observe polygonal terrain on the vast volcanic areas of the Martian highlands such as Lunae Planum or Syrtis Major or on the young flows of the large shield volcanoes. On the basis of these observations we conclude that large-scale polygonal terrain in Utopia Planitia most likely formed on sediments, rather than volcanic substrates.

Which process formed giant polygonal terrain in southern Utopia Planitia? Volcanic models: Besides the general objections to a volcanic origin of giant polygonal terrain described above, there are additional specific arguments against volcanic models. MOLA data show that formation of polygonal terrain due to basalt loading onto water-saturated sediments can be clearly ruled out because Martian polygons are bounded by troughs instead of ridges as proposed in the model by *Needham* [1978]. Cooling of a basalt flow would produce small-scale fractures near the surface [*Pechmann*, 1980] but MOLA and MOC data indicate that the majority of troughs is rather wide and deep and do not resemble small-scale fractures known from basalt flows on Earth. Also, Martian polygonal troughs are poorly interconnected, whereas polygonal fracture patterns on terrestrial lava flows usually show well-defined T, curved T, and Y intersections [*Aydin and DeGraff*, 1988]. *Pechmann* [1980] also noted that cooling of volcanic flows would form a large number of small fractures, but inspection of MOC images showed no evidence for such features. In addition giant polygonal terrain on volcanic flows is unknown from volcanic provinces on other terrestrial planets such as Earth and the Moon. Only on Venus, which is almost entirely covered with volcanic material, do a few very small and locally confined areas show giant polygons. Provided the Venusian polygons were formed by cooling cracks as suggested by *Johnson and Sandwell* [1992] why are they limited to small areas and are not distributed globally, that is, on all the other Venusian volcanic plains? In addition, from the observation that these polygons are in close vicinity to coronae structures we conclude that they are more likely to be tectonic in origin. From the similarity to Venusian polygons we conclude that a tectonic process could also have formed giant polygons on Mars or other planets.

Sedimentary models: A major argument against a formation of polygonal terrain related to desiccation of wet sediments is the size of Martian polygons and the depth of the associated troughs [*Pechmann*, 1980]. MOLA data show that 69% of the troughs are more than 20 m deep and 38% are more than 30 m deep. The maximum depth measured in the MOLA profiles is of the order of 110 m. MOC images show that the troughs are filled with aeolian deposits indicating that the troughs were originally even deeper. We conclude that a large number of troughs exhibit depths which exceed Pechmann's upper limit of 15-20 m for the stability of vertical tension cracks on Mars [*Pechmann*, 1980]. To our knowledge, terrestrial desiccation cracks are commonly highly interconnected, but Viking and MOC images show that giant polygons are poorly interconnected.

Not to be confused with the formation process of giant polygons is the origin of small-scale polygons. In some MOC images we observed small-scale polygons on the fluidized ejecta blankets of impact craters which are superposed on giant polygonal terrain. Craters with fluidized ejecta are interpreted to have formed in volatile-rich substrates [e.g., *Squyres et al.*, 1992; *Cave*, 1993; *Costard and Kargel*, 1995], and thus these small polygons are likely to have formed when a wet ejecta blanket desiccated. An alternative process for the formation of these small polygons is thermal contraction of a cooling ejecta blanket as discussed below.

Pechmann [1980] noted that thermal contraction is confined to the uppermost 10 m of the surface and can not produce deep fractures. MOLA data show that numerous troughs of giant polygons are deeper than 10 m. Again, from the statistical distribution of trough depths seen in the MOLA data we conclude that the observed depths seem to be too deep as to be formed by thermal contraction. If Pechmann's calculations are correct we have to reject this formation hypothesis at the present state of knowledge. In addition, thermal contraction cracks have to be widened by repeated frost-cracking cycles, that is, ice-wedging processes, in order to match the observed trough widths. However, there is no evidence (e.g., common raised rims) for such a process in the MOC images. *Pechmann* [1980] noted that flat-floored steep-sided cross sections are difficult to explain with thermal contraction. However, both Viking and MOC data yield unambiguous evidence for such flat-floored steep-sided trough morphology.

Small-scale polygons similar in size to polygons formed by thermal contraction in permafrost on Earth were observed on the fluidized ejecta blankets of craters, which are younger than giant polygonal terrain. These smaller polygons are far more interconnected, show raised rims, and flat trough floors are rare. Therefore a formation of these small polygons by thermal contraction of a cooling ejecta blanket may be possible.

Coalescence of smaller polygons, which formed by ice wedging, is unlikely. In this model, initial troughs are primarily formed by ice wedging, that is, thermal contraction, and Pechmann's argument against such a formation process is that it is difficult to explain a flat-floored steep-sided trough cross section. Coalescence of small polygons would then form giant polygons by a desiccation process [*Helfenstein and Mouginis-Mark*, 1980]. Meandering of the polygonal troughs was interpreted as evidence for coalescence of smaller polygons [*Helfenstein and Mouginis-Mark*, 1980] but is not a definitive characteristic and may be simply the result of crack development and en echelon propagation as described by *Beloussov* [1962] and *Johnson and Sandwell* [1992]. MOC images show that the troughs are graben-like features and do not exhibit raised rims as would be expected if ice wedging was the dominant process. Most important, in the MOC images (Figures 11 and 13) we do not see small-scale polygons within the giant polygons. From our observations we conclude that coalescence of smaller polygons is not likely to form giant polygons.

Tectonic models: Formation of polygonal faults in response of compaction due to dewatering of wet sediments was proposed for terrestrial polygons by *Cartwright and Lonergan* [1996], *Lonergan et al.* [1998], *Lonergan and Cartwright* [1999], and *Cartwright and Dewhurst* [1998]. However, the size of the terrestrial polygons is up to 1 km and therefore considerably smaller than Martian polygons. Also terrestrial polygonal faults are highly interconnected, whereas Martian polygons are not. In addition, these terrestrial polygons are bound by normal faults, whereas MOC images show that Martian polygons are outlined by graben. To form the polygonal faults on Earth, a shallow burial of <1000 m is required. If this process was active on Mars then it would imply that this sediment layer had to be stripped off in order to make the polygons visible.

If we assume a formation related to differential compaction,

which would cause bending of the compacting layer over preexisting topography, polygons would preferentially occur above topographic highs [*McGill and Hills*, 1992]. Convection models [*Wenrich and Christensen*, 1993, 1996] also predict the formation of troughs above topographic highs where tensile stress induced by bending is predicted to be larger. MOLA data show that some polygonal fractures can occur over local topographic highs. However, most of the troughs are not located above topographic highs and must therefore be formed by a different process.

Such a process could be uplift of the floor of the Utopia basin. Tectonic uplift of a basin floor causing the formation of polygonal terrain was proposed for the Caloris basin on Mercury [*Strom et al.*, 1975], and uplift of crater floors is frequently observed on the Moon causing the formation of fractures on crater floors [*Schultz*, 1976; *Hall et al.*, 1981]. For the Caloris basin it is inferred that tectonic uplift can produce polygons with sizes comparable to the Martian giant polygons. In the MOLA data we made the observation that trough depths increase toward the basin center, the area with potentially the largest uplift. A tectonic formation of polygonal terrain is further supported by the flat-floored graben-like appearance of the troughs in the MOC images. Trough rims appear sharp and primary and there is but little evidence for wall erosion and scarp retreat related infilling. Giant polygons in southern Utopia Planitia do not exhibit raised rims in the MOC images but marginal terraces are frequently observed. Such terraces are interpreted to be the result of normal faulting related to the graben formation associated with the postulated uplift of the basin center.

What might be the cause of uplift? Numerous authors have proposed that the Utopia basin once contained ponded water [e.g., *Scott et al.*, 1992; *Chapman*, 1994; *DeHon*, 1992; *Thomson and Head*, 1999]. Furthermore, the Utopia basin itself is located within the shorelines of a proposed north polar ocean [*Parker et al.*, 1989, 1993] and northern plains ice sheet [*Kargel et al.*, 1995]. *Head et al.* [1998, 1999] used MOLA data to test for the existence of this ocean and their results are consistent with a large standing body of water within the northern lowlands. Independent evidence for large amounts of volatiles in this area comes from superposed craters with lobate ejecta blankets which were interpreted as impacts into a water/ice rich substrate [e.g., *Squyres et al.*, 1992; *Cave*, 1993; *Costard and Kargel*, 1995]. *Thomson and Head* [1999] calculated the volume of water that could have been contained in the Utopia basin prior to spilling into adjacent low-lying areas. Their calculations show that the Utopia basin could hold as much as 1.2 x 10^6 km^3 of water with a maximum depth of ~650 m. Assuming a diameter of the Utopia basin of 2100 km [*Thomson and Head*, 1999] the average thickness of the water layer in the Utopia basin would be ~350 m. *Parker et al.* [1989, 1993] mapped two possible shorelines of a north polar ocean and *Head et al.* [1999] found that the mean elevation of the younger shoreline, Contact 2, at an elevation of -3760 m, is a reasonable approximation to an equipotential surface. Provided that at some point in Martian history this north polar ocean filled the northern lowlands up to Contact 2, an additional water layer of 600 m thickness would have covered the Utopia basin.

Summing up these numbers yields a thickness of the water layer of almost 1 km which, for comparison, is within the range of thicknesses of the Laurentide ice shield (~300-3000 m) and the Scandinavian ice shield (~3000 m) [*Flint*, 1971]. It is well known that terrestrial areas that were formerly covered with ice are currently updoming due to unloading (Figure 16). Contemporary uplift rates are of the order of up to 5 mm/y in North America and up to 9 mm/y in Scandinavia [*Flint*, 1971]. It is assumed that uplift rates were even larger immediately after deglaciation. In order to estimate the amount of total uplift after deglaciation on Earth the elevation of ancient beaches are measured relative to the present sea level and corrected for meteorologic and other extraneous effects. In the area of the Hudson Bay uplift was of the order of 275 m over the last 10,000 years and for Fennoscandia uplift was about 520 m. For Fennoscandia, additional future uplift of 210 m is expected, for a total of 730 m. According to *Mörner* [1980], the total amount of uplift in Sweden was in excess of 700 m. It is calculated that the Hudson Bay area should rise ~100-250 m more before crustal recovery is complete [*Flint*, 1971]. Uplift began immediately after deglaciation but displacement of the glacier margin had to occur, permitting a lake to occupy part of the area formerly covered with ice before the formation of a shoreline could start. This early uplift constituted as much as half of the total uplift which is of the order of 1 km for the Laurentide ice shield [*Flint*, 1971].

Uplift of the order of 1 km on Mars would cause extension of the surface of 0.03% [*Pechmann*, 1980]. In order to test the plausibility of a formation of polygons due to uplift of the basin floor we estimated the possible extension represented by the polygonal troughs in Utopia. As described earlier, calculations of strain by measuring the trough width in relation to profile length can be influenced by erosional widening of the troughs. For this reason our calculations are based on observations of lunar graben which suggest dip angles of 60° [*McGill*, 1971; *Golombek*, 1979]. Based on observations that normal faults in homogeneous materials generally have dip angles around 60°, *Pechmann* [1980] calculated that for a typical trough depth of 80 m, a trough spacing of 5-10 km and dip angles of 60° and 80°, the extension would be of the order of 1-2% and 0.3-0.6%, respectively. He concluded that the fault dips must be significantly larger than 60° if polygons are formed by updoming. Taking into account the new trough depths of ~30 m derived from MOLA, we find that at a dip angle of 60° the extension is 0.2-0.3% and at 80° it is about 0.05-0.1%, a value very similar to the extension that could be produced by a 1 km uplift of the Utopia basin floor. We conclude that the removal of a former standing body of water/ice in Utopia Planitia may be sufficient to initiate some tectonic uplift which itself could cause the formation of polygonal terrain. In addition, freezing and expansion of sediment-mantled ice-covered water, or a water-saturated subsurface, could add to uplift and expansion and may have contributed to the formation of large polygons.

6. Conclusions

Small-scale polygons in Utopia Planitia are restricted to fluidized ejecta blankets of young impact craters and may have formed by desiccation and/or thermal contraction. Results from MOLA and MOC data show, however, that large polygons differ in many significant ways. We interpret these new data to be consistent with formation of giant polygons in the area of a paleolake that once filled the Utopia basin. We note that the distribution of polygonal terrain is closely related to the Utopia basin, a region that is interpreted to have accumulated water, ice, and sediment during the formation of at least temporarily standing bodies of water. We propose that the polygons are primarily of tectonic origin, being caused by uplift of the

floor of the Utopia basin following removal of the later/ice load. Evidence for this hypothesis is that (1) the polygons appear to be outlined by graben, (2) that the polygons are too large to be related simply to desiccation and contraction, (3) that the polygons are of similar scale to polygons on the floor of the Caloris basin on Mercury, interpreted to be due to tectonic uplift by *Strom et al.* [1975], and (4) that the troughs increase in depth toward the basin center, perhaps correlating with maximum uplift.

Where is the origin of the uplift? We believe that the removal of the load representing former standing bodies of water is a good candidate. Water thickness estimated in these areas is ~1 km. This thickness is comparable to the loads placed on terrestrial continental lithosphere by the Laurentide and Scandinavian ice sheets. We hypothesize that removal of this load by loss of the water or ice could cause uplift of the floor and polygon formation. Freezing and expansion of incompletely solidified sediment-covered ice layers could also contribute to this effect. From the discussion of the different models in the light of the MOLA and MOC data we conclude that a formation of giant polygons by tectonic uplift of the basin floor is likely and deserves further investigation.

Acknowledgments. We gratefully acknowledge the superb work of the MOLA design, engineering, and altimetry processing team and the NASA Mars Global Surveyor Project, who funded this work. We also gratefully acknowledge Malin Space Science Systems for the design and engineering of the Mars Orbiter Camera, and for the mission planning, data acquisition, and processing of the excellent MOC images that were an important part of this analysis. Thanks are also extended to Anne Côté, Steve Pratt, and Nancy Carroll for help in manuscript preparation.

References

Allen, J. R. L., *Principles of Physical Sedimentology*, Allen and Unwin, Winchester, Mass., 1985.

Aydin, A., and J. M. DeGraff, Evolution of polygonal fracture patterns in lava flows, *Science, 239*, 471-476, 1988.

Barlow, N., Sinuosity of Martian rampart ejecta deposits, *J. Geophys. Res., 99*, 10,927-10,935, 1994.

Barnouin-Jah, O., and P. H. Schultz, Lobateness of impact ejecta deposits from atmospheric interactions, *J. Geophys. Res., 103*, 25,739-25,756, 1998.

Beloussov, V. V., *Basic Problems in Geotectonics*, 816 pp., McGraw-Hill, New York, 1962.

Black, R. F., Comparison of some permafrost features on Earth and Mars: Some cautions and restrictions, in *Proceedings of the Second Colloquium on Planetary Water and Polar Processes*, pp. 127-130, U.S. Army, Cold Reg. Res. and Eng. Lab., Hanover, N. H., 1978.

Blasius, K. R., J. A. Cutts, J. E. Guest, and H. Masursky, Geology of the Valles Marineris: First analysis of imaging from the Viking 1 orbiter primary mission, *J. Geophys. Res., 82*, 4067-4091, 1977.

Borrello, M. C., Surficial and structural analysis of large patterned fractures in Southern Acidalia Planitia, Mars (abstract), *Lunar Planet. Sci., XVIII*, 107-108, 1987.

Carr, M. H., *Water on Mars*, 229 pp., Oxford Univ. Press, New York, 1996.

Carr, M. H., and G. G. Schaber, Martian permafrost features, *J. Geophys. Res., 82*, 4039-4054, 1977.

Carr, M. H., H. Masursky, W. A. Baum, K. R. Blasius, G. A. Briggs, J. A. Cutts, T. Duxburry, R. Greeley, J. E. Guest, B. A. Smith, L. A. Soderblom, J. Veverka, and J. B. Wellman, Preliminary results from the Viking orbiter imaging experiment, *Science, 193*, 766-776, 1976.

Carr, M. H., L. S. Crumpler, J. A. Cutts, R. Greeley, J. E. Guest, and H. Masursky, Martian impact craters and emplacement of ejecta by surface flow, *J. Geophys. Res., 82*, 4055-4065, 1977.

Cartwright, J. A., and D. N. Dewhurst, Layer-bound compaction faults in fine-grained sediments, *Geol. Soc. Am. Bull., 110*, 1242-1257, 1998.

Cartwright, J. A., and L. Lonergan, Volumetric contraction during the compaction of mudrocks: A mechanism for the development of regional-scale polygonal fault systems, *Basin Res., 8*, 183-193, 1996.

Cave, J., Ice in the northern lowlands and southern highlands of Mars and its enrichment beneath the Elysium lavas, *J. Geophys. Res., 98*, 11,079-11,097, 1993.

Chapman, M. G., Evidence, age, and thickness of a frozen paleolake in Utopia Planitia, Mars, *Icarus, 109*, 393-406, 1994.

Christiansen, E. H., Lahars in the Elysium region of Mars, *Geology, 17*, 203-206, 1989.

Corte, A. E., Relationship between four ground patterns, structure of the active layer, and type and distribution of ice in the permafrost, *Biul. Periglacial. 12*, 8-86, 1963.

Costard, F. M., and J. S. Kargel, Outwash plains and thermokarst on Mars, *Icarus, 114*, 93-112, 1995.

DeHon, R. A., Martian lake basins and lacustrine plains, *Earth Moon Planets, 56*, 95-122, 1992.

Eliason, E., R. Batson, and A. Manley, Mars mosaicked digital image model (MDIM) and digital terrain model (DTM), in *Mission to Mars, [CD-ROM], vol. 7*, U.S. Geol. Surv., Flagstaff, Ariz., 1992.

Flint, R. F., *Glacial and Quaternary Geology*, 892 pp., John Wiley, New York, 1971.

Frey, H. V., and R. A Schultz, Speculations on the origin and evolution of the Utopia-Elysium lowlands of Mars, *J. Geophys. Res., 95*, 14,203-14,213, 1990.

Golombek, M. P., Structural analysis of lunar grabens and the shallow crustal structure of the Moon, *J. Geophys. Res., 84*, 4657-4666, 1979.

Greeley, R., and J. E. Guest, Geologic map of the eastern equatorial region of Mars, 1:15,000,000, *U.S. Geol. Surv. Misc. Invest. Ser. Map I-1802-B*, 1987.

Hall, J. L., S. C. Solomon, and J. W. Head III, Lunar floor-fractured craters: Evidence for viscous relaxation of crater topography, *J. Geophys. Res., 86*, 9537-9552, 1981.

Head, J. W., M. Kreslavsky, M. Ivanov, H. Hiesinger, S. Pratt, N. Seibert, D. E. Smith, and M. T. Zuber, Oceans in the past history of Mars: Tests for their presence using Mars Orbiter Laser Altimeter (MOLA) data, *Geophys. Res. Lett., 25*, NO.24, 4401-4404, 1998.

Head, J. W., H. Hiesinger, M. A. Ivanov, M. A. Kreslavsky, S. Pratt, and B. J. Thomson, Possible ancient oceans on Mars: Evidence from Mars Orbiter Laser Altimeter data, *Science, 286*, 2134-2137, 1999.

Helfenstein, P., and P. J. Mouginis-Mark, Morphology and distribution of fractured terrain on Mars (abstract), *Lunar Planet. Sci., XI*, 429-431, 1980.

Higgins, C. G., D. R. Coates, T. L. Péwé, R. A. M. Schmidt, and C. E. Sloan, Permafrost and thermokarst: Geomorphic effects of subsurface water on landforms of cold regions, *Spec. Pap. Geol. Soc. Am. , 252*, 211-218, 1990.

Hobbs, P. V., *Ice Physics*, 837pp., Clarendon, Oxford, England, 1974.

Johnson, C. L., and D. T. Sandwell, Joints in Venusian lava flows, *J. Geophys. Res., 97*, 13,601-13,610, 1992.

Kargel, J. S., V. R. Baker, J. E. Begét, J. F. Lockwood, T. L. Péwé, J. S. Shaw, and R. G. Strom, Evidence of continental glaciation in the Martian northern plains, *J. Geophys. Res., 100*, 5351-5368, 1995.

Kuzmin, R. O., N. N. Bobina, E. V. Zabalueva, and V. P. Shashkina, Inhomogeneities in the upper levels of Martian cryo-lithosphere (abstract), *Lunar Planet. Sci., XIX*, 655-656, 1988a.

Kuzmin, R. O., N. N. Bobina, E. V. Zabalueva, and V. P. Shashkina, Mars: Estimation of the relative ice content in upper layers of the permafrost (abstract), *Lunar Planet. Sci., XIX*, 657-658, 1988b.

Lachenbruch, A. H., Mechanics of thermal contraction cracks and ice-wedge polygons in permafrost, *Spec. Pap. Geol. Soc. Am., 70*, pp. 68, 1962.

Lonergan, L., and J. Cartwright, Polygonal faults and their influence on deep-water sandstone reservoir geometries, Alba Field, United Kingdom central North Sea, *AAPG Bull., 83*, 410-432, 1999.

Lonergan, L., J. Cartwright, and R. Jolly, The geometry of polygonal fault systems in Tertiary mudrocks of the North Sea, *J. Struct. Geol., 20*, 529-548, 1998.

Lucchitta, B. K., Permafrost on Mars: Polygonally fractured ground, in *Permafrost: Proceedings of the. 4th International Conference*, pp. 744-748, Nat. Acad. Press, Washington, D.C., 1983.

Lucchitta, B. K., H. M. Ferguson, and C. Summers, Sedimentary deposits in the northern lowland plains, Mars, *Proc. Lunar Planet. Sci. Conf. 17th*, Part 1, *J. Geophys. Res., 91*, suppl., E166-E174, 1986.

Malin, M. C., M. H. Carr, G. E. Danielson, M. E. Davies, W. K. Hartmann, A. P. Ingersoll, P. B. James, H. Masursky, A. S. McEwen, L. A. Soderblom, P. Thomas, J. Veverka, M. A. Caplinger, M. A. Ravine, T. A. Soulanille, and J. L. Warren, Early views of the Martian surface from the Mars Orbiter Camera of Mars Global Surveyor, *Science, 279*, 1681-1685, 1998.

Masursky, H., and N. L. Grabill, Search for the Viking 2 landing site, *Science, 194*, 62-68, 1976.

McGill, G. E., Attitude of fractures bounding straight and arcuate lunar rilles, *Icarus, 14*, 53-58, 1971.

McGill, G. E., The giant polygons of Utopia, northern Martian plains, *Geophys. Res. Lett., 13*, 705-708, 1986.

McGill, G. E., Constraints on the origin of fractured terrane, northern Martian plains, in *MEVTV Workshop on Nature and Composition of Surface Units on Mars, LPI Tech. Rep., 88-05*, Lunar and Planet. Inst., Houston, Tex., 1987.

McGill, G. E., Buried topography of Utopia, Mars: Persistence of a giant impact depression, *J. Geophys. Res., 94*, 2753-2759, 1989.

McGill, G. E., and L. S. Hills, Origin of giant Martian polygons, *J. Geophys. Res., 97*, 2633-2647, 1992.

Mörner, N. A. (Ed.), The Fennoscandian uplift: Geological data and their geodynamical implications, in *Earth Rheology, Isostacy, and Eustacy*, pp. 251-284, John Wiley, New York, 1980.

Morris, E. C., and J. R. Underwood, Polygonal fractures of Martian plains, *NASA Tech. Memo., 79729*, 97-99, 1978.

Mouginis-Mark, P., Martian fluidized crater morphology: Variations with crater size, latitude, altitude, and target material, *J. Geophys. Res., 84*, 8011-8022, 1979.

Mouginis-Mark, P., Ejecta emplacement and modes of formation of Martian fluidized ejecta craters, *Icarus, 45*, 60-76, 1981.

Mouginis-Mark, P., Ice or liquid water in the Martian regolith? Morphologic indicators from rampart craters, *LPI Tech. Rep. 87-01*, pp. 81-83, Lunar and Planet. Inst., Houston, Tex., 1986.

Müller, G., Starch columns: Analog model for basalt columns, *J. Geophys. Res., 103*, 15,239-15,253, 1998.

Mutch, T. A., R. E. Arvidson, J. W. Head III, K. L. Jones, and R. S. Saunders, *The Geology of Mars*, Princeton Univ. Press, Princeton, N. J., 1976.

Neal, J. T., A. M. Langer, and P. F. Kerr, Giant desiccation polygons of Great Basin playas, *Geol. Soc. Am. Bull., 79*, 69-90, 1968.

Needham, R. S., Giant-scale hydroplastic deformation structures formed by the loading of basalt onto water-saturated sand, Middle Proterozoic, Northern Territory, Australia, *Sedimentology, 25*, 285-295, 1978.

Parker, T. J., R. S. Saunders, and D. M. Schneeberger, Transitional morphology in West Deuteronilus Mensae, Mars: Implications for modification of the Lowland/Upland boundary, *Icarus, 82*, 111-145, 1989.

Parker, T. J., D. S. Gorsline, R. S. Saunders, D. C. Pieri, and D. M. Schneeberger, Coastal geomorphology of the Martian northern plains, *J. Geophys. Res., 98*, 11,061-11,078, 1993.

Pechmann, J. C., The origin of polygonal troughs on the northern plains of Mars, *Icarus, 42*, 185-210, 1980.

Pike, R. J., and P. A. Davis, Toward a topographic model of Martian craters from photoclinometry (abstract), *Lunar Planet. Sci., XV*, 645-646, 1984.

Ross, R. G., and J. S. Kargel, Thermal conductivity of solar system ices, with special reference to Martian polar caps, in *Solar System Ices, vol. 27, Astrophysics and Space Library*, (edited by B. Schmitt, C. De Bergh, and M. Festou), pp. 33-63, Kluwer Acad., Norwell, Mass., 1998.

Schultz, P. H., Floor-fractured lunar craters, *Moon, 15*, 241-273, 1976.

Schultz, P. H., and D. E. Gault, Atmospheric effects on Martian ejecta emplacement, *J. Geophys. Res., 84*, 7669-7687, 1979.

Schultz, R. A., and H. V. Frey, A new survey of large multiring basins on Mars, *J. Geophys. Res., 95*, 14,175-14,189, 1990.

Scott, D. H., and K. L. Tanaka, Geologic map of the western equatorial regions of Mars, *U.S. Geol. Surv. Misc. Invest. Ser. Map I-1802-A*, 1986.

Scott, D. H., J. M. Dohm, and J. W. Rice Jr., Map of Mars showing channels and possible paleolake basins, *U.S. Geol. Surv. Misc. Invest. Ser. Map I-2461*, 1992.

Sleep, N. H., Martian plate tectonics, *Eos Trans., AGU, 74* (43), Fall Meet. Suppl., 382, 1993.

Smith, D. E., M. T. Zuber, H. V. Frey, J. B. Garvin, J. W. Head, D. O. Muhleman, G. H. Pettengill, R. J. Phillips, S. C. Solomon, H. J. Zwally, W. B. Banerdt, and T. C. Duxbury, Topography of the northern hemisphere of Mars from the Mars Orbiter Laser Altimeter, *Science, 279*, 1686-1691, 1998.

Smith, D. E., M. T. Zuber, S. C. Solomon, R. J. Phillips, J. W. Head, J. B. Garvin, W. B. Banerdt, D. O. Muhleman, G. H. Pettengill, G. A. Neumann, F. G. Lemoine, J. B. Abshire, O. Aharonson, C. D. Brown, S. A. Hauck, A. B. Ivanov, P. J. McGovern, H. J. Zwally, and T. C. Duxbury, The global topography of Mars and implications for surface evolution, *Science, 284*, 1495-1503, 1999.

Squyres S. W., S. M. Clifford, R. O. Kuzmin, J. R. Zimbelman, and F. Costard, Volatiles in the Martian regolith, in *Mars* , edited by H. H. Kieffer et al., pp. 523-554, Univ. Arizona Press, Tucson, Ariz., 1992.

Strom, R. G., N. J. Trask, and J. E. Guest, Tectonism and volcanism on Mercury, *J. Geophys. Res., 80*, 2478-2507, 1975.

Tanaka, K. L., and P. A. Davis, Tectonic history of the Syria Planum province of Mars, *J. Geophys. Res., 93*, 12,893-12,917, 1988.

Thomson, B., and J. W. Head III, Utopia basin, Mars: A new assessment using Mars Orbiter Laser Altimeter (MOLA) data (abstract), *Lunar Planet. Sci., XXX*, [CD-ROM 1894], 1999.

Weinberger, R., Initiation and growth of cracks during desiccation of stratified muddy sediments, *J. Struct. Geol., 21*, 379-386, 1999.

Wenrich, M. L., and P. R. Christensen, A formational model for the polygonal terrains of Mars: Taking a "crack" at the genesis of the Martian polygons, *LPI Tech. Rep., 93-04, Part 1*, pp. 19-21, Lunar and Planet. Inst., Houston, Tex., 1993.

Wenrich, M. L., and P. R. Christensen, A formational model for the Martian polygonal terrains (abstract), *Lunar Planet. Sci., XXVII*, 1419-1420, 1996.

Zuber, M. T., D. E. Smith, S. C. Solomon, J. B. Abshire, R. S. Afzal, O. Aharonson, K. Fishbaugh, P. G. Ford, H. V. Frey, J. B. Garvin, J. W. Head, A. B. Ivanov, C. L. Johnson, D. O. Muhleman, G. A. Neumann, G. H. Pettengill, R. J. Phillips, X. Sun, H. J. Zwally, W. B. Banerdt, and T. C. Duxbury, Observations of the North Polar region of Mars from the Mars Orbiter Laser Altimeter, *Science, 282*, 2053-2060, 1998.

H. Hiesinger and J. W. Head III, Department of Geological Sciences, Brown University, Box 1846, Providence, RI 02912. (Harald_Hiesinger@Brown.edu)

(Received September 30, 1999; revised February 22, 2000;
Accepted February 29, 2000.)